

## *RESULTS and DISCUSSION*

## CHAPTER THREE

### Results and Discussions

#### 3.1 Effect of Sodium Content on the Electrical Properties of Silicate Based Glasses

##### 3.1.1 The Temperature dependence of D.C conductivity

The dependence of the D.C electrical conductivity on the reciprocal of absolute temperature for the glassy samples [X (Na<sub>2</sub>O). 0.53(SiO<sub>2</sub>). 0.08(Bi<sub>2</sub>O<sub>3</sub>). (0.39-X)(B<sub>2</sub>O<sub>3</sub>)], where X = 0.05(S1), 0.15(S2), 0.25(S3) and 0.35(S4) were studied over the temperature range (400-850) K and is shown in Fig. (3.1). The data show that the conductivity is slightly increased from room temperature up to different transition temperature as shown in table (3.1), after that, a large increase of  $\sigma_{dc}$  is obvious because of the thermal energy. The data in the figure obeys the Arrhenius relation<sup>(72)</sup> for ionic diffusion.

$$\sigma_{dc} T = \sigma' \exp (-E_{dc} / kT) \quad (3-1)$$

where ( $\sigma'$ ) is a pre-exponential factor as composition and temperature dependent, (k) is the Boltzmann's constant, (T) is the absolute temperature and ( $E_{dc}$ ) is the activation energy for the dc conduction. From the figure, it is also clear that there are two straight lines with two different slopes and different activation energies separated by the transition point. The value of the activation energy is calculated by using least square method from the experimental data of DC conductivity for the different samples are listed in table (3.1).

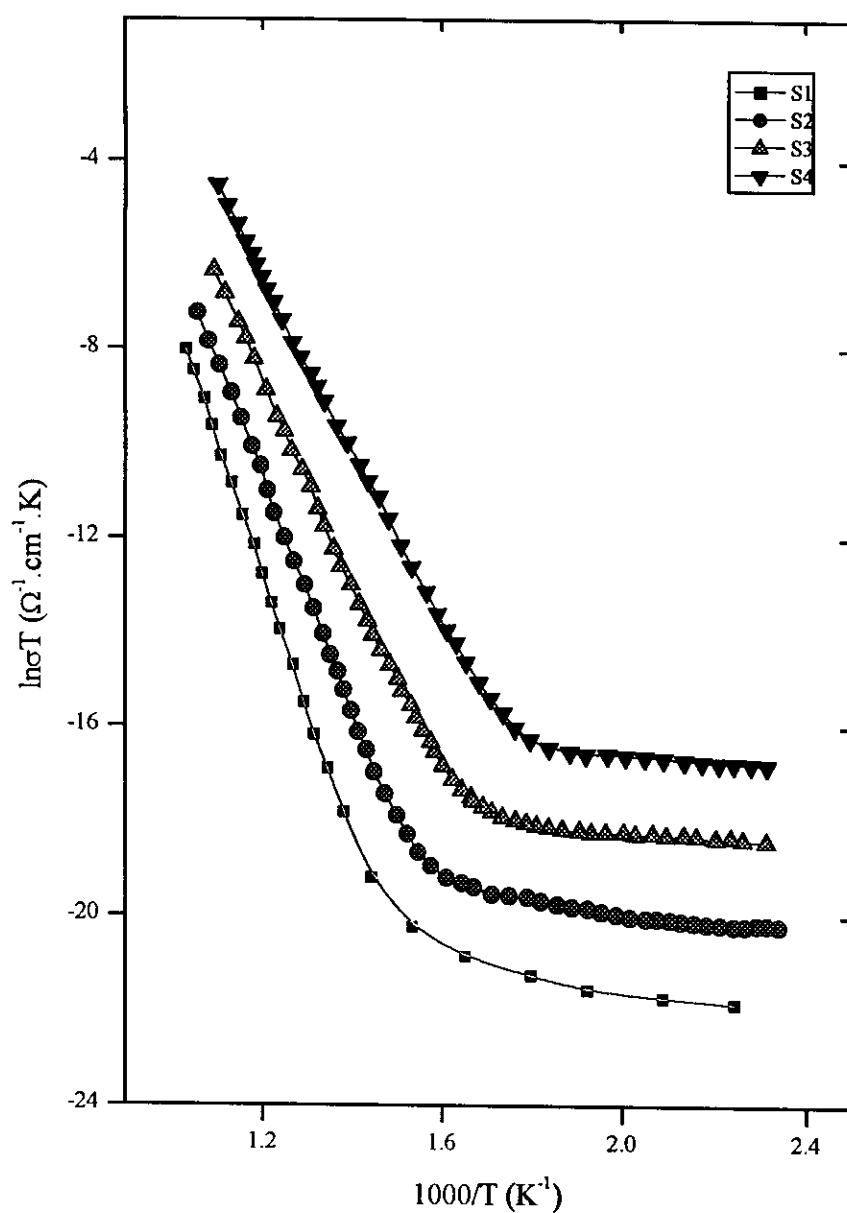


Fig. (3.1): Dependence of DC conductivity on the reciprocal of temperature for the samples  $x\text{Na}_2\text{O}$ ,  $53\text{SiO}_2$ ,  $39-x\text{B}_2\text{O}_3$ ,  $8\text{Bi}_2\text{O}_3$ ;  $X=5$ (S1),  $15$ (S2),  $25$ (S3) and  $35$ (S4).

The increase in the DC conductivity can be ascribed to the increase in the mobility of charge carriers (electrons, ions or both) in cooperation with each other. While the hopping length of electrons and the diffusion length of ions increased with increasing thermal energy, which activates more charge carriers to participate in the conduction process. In other words, the thermal energy will move the  $\text{Na}^+$  ions from one place to another to enhance the conduction mechanism.

Many authors explained the ionic conductivity in binary silicate glass with alkali ions <sup>(93)</sup>, which is similar to the investigated samples. The two straight lines appeared in the figure indicate the different conduction mechanisms. One of these mechanisms that can be suggested is the small polaron model <sup>(1)</sup>, which plays a role simultaneously with the collective behavior of the alkali ion contained in the sample. This is because the sample containing sodium ions is characterized by a phonon like behavior of very large wavelength <sup>(94)</sup>.

In other words, one can say that, the conductivity depends on the concentration of the glass constituent as well as the motion of the polaron through the material because the thermal energy will help the conduction in the sample. So one can expect an increase in the conductivity with increasing temperature. The obtained data enhances such expectation.

The correlated – barrier hopping model <sup>(1)</sup> is the second model of conduction, which suggests that the electrons in the n-type behavior or holes in the p-type behavior can jump between the different states <sup>(34)</sup>, from filled to empty states. On these states, the alkali element is not interacting only with one of non bridging oxygen but it can interact with

non-bridging oxygen of its nearest neighbor. This can reflect the fact that the non-bridging oxygen plays a significant role in the conductivity.

From a closer look to the data in the table, one can find that the activation energy at the low temperature region is less than that in the high temperature region. This was an acceptable result because in the high temperature region the thermal energy is quite large to move the ions to participation in the conduction processes.

From a general scope of the samples, the conductivity of the present glasses depends markedly on the amount of sodium ions ( $\text{Na}^+$ ) present in the system, i.e. the higher the sodium concentration, the larger values of the conductivity. This is also reflected in the values of the activation energy for all the investigated glasses. Due to the interconnected structure of the glasses <sup>(31)</sup>, the electrical conductivity is expressed vein of the sodium-rich phase.

The dependence of the temperature breaks on the composition of the glassy samples is listed in table (3.1) that, referred to the presence of different electrostatic forces between each of the framework units and the sodium modifier ions as well as the dependence of the relaxation of the framework on the composition. Generally by comparing  $E_{dc}$  in the very low range of temperature, we can observe that  $E_{dc}$  decreases with increasing sodium ions content in the sample due to increasing the electrostatic forces between the framework and sodium ions <sup>(93)</sup>.

On the basis of the high concentrations of  $\text{Na}^+$  ions and their existence in the interstitial positions as modifiers for the framework of

borate and silicate oxide in the glasses. Anderson's model <sup>(31)</sup> will be considered to explain the conduction of the ionic migration of  $\text{Na}^+$  ions. According to this model, the activation energy for conduction process is considered as the summation of two terms  $E_a = E_b + E_s$ , where  $E_b$  is the energy required to overcome electrostatic forces and  $E_s$  is the energy required to open up "doorways" in the structure large enough for the ions to pass through it "strain energies". Thus, the rise of temperature leads to the release of some of the stored strains in the glass structure. This enhances the opening of such doorways and subsequently increases the probability of  $\text{Na}^+$  ion migration to the new sites. Both activation energies are composition dependent, which also may be expected on the basis that the conduction process occurring mainly due to the hopping of  $\text{Na}^+$  ion in the glass matrix.

Table (3.1): The D.C activation energy at low ( $E_I$ ), high ( $E_{II}$ ) temperature and the transition temperature of the samples X ( $\text{Na}_2\text{O}$ ). 0.53( $\text{SiO}_2$ ). 0.08( $\text{Bi}_2\text{O}_3$ ). (0.39-X)( $\text{B}_2\text{O}_3$ ); X = 0.05(S1), 0.15(S2), 0.25(S3), 0.35(S4).

Sample No.	$E_I$ (eV)	$E_{II}$ (eV)	Transition Temperature (K)
S1	0.16	0.91	633
S2	0.10	0.86	625
S3	0.03	0.76	588
S4	0.02	0.52	555

The D.C electrical conductivity after ionic exchange by silver ions, with the time of ion exchange (12, 24, 36, and 48 h) for different glassy samples, was studied over the temperature range (300-830) K. Fig. (3.2), correlates the D.C conductivity and reciprocal of absolute temperature. After ion exchange a slight increase in the conductivity from room temperature up to nearly 500 K is observed after that a large increase in  $\sigma$  is obvious as a result of the thermal energy. From the figure, it is clear that two straight lines with two different slopes and two different activation energies separated by the transition region are obtained. The value of activation energy is calculated by using least square method from the relation (3.1) and reported in table (3.2)

The increase in the dc conductivity can be ascribed to the increase in the mobility of charge carriers not to the increase in their number. This can be due to the variation in the hopping length of electrons, hence the diffusion length of ions are increased with increasing thermal energy. So the increase in the hopping length can not lead to the increase in the conductivity.

Generally, the activation energy depended markedly on the sodium content as in table (3.2). This is also reflected in the values of the activation energy that relatively changed by increasing the time of ion exchange for the glassy samples. The high conduction state induced in the ion exchanged glasses is ascribed for the enhancement of the growth rate of the silver rich phase <sup>(31)</sup> due to applying electric field in the presence of thermal energy. Hence, the electrical conductivity is essentially determined by that of the silver - rich phase.

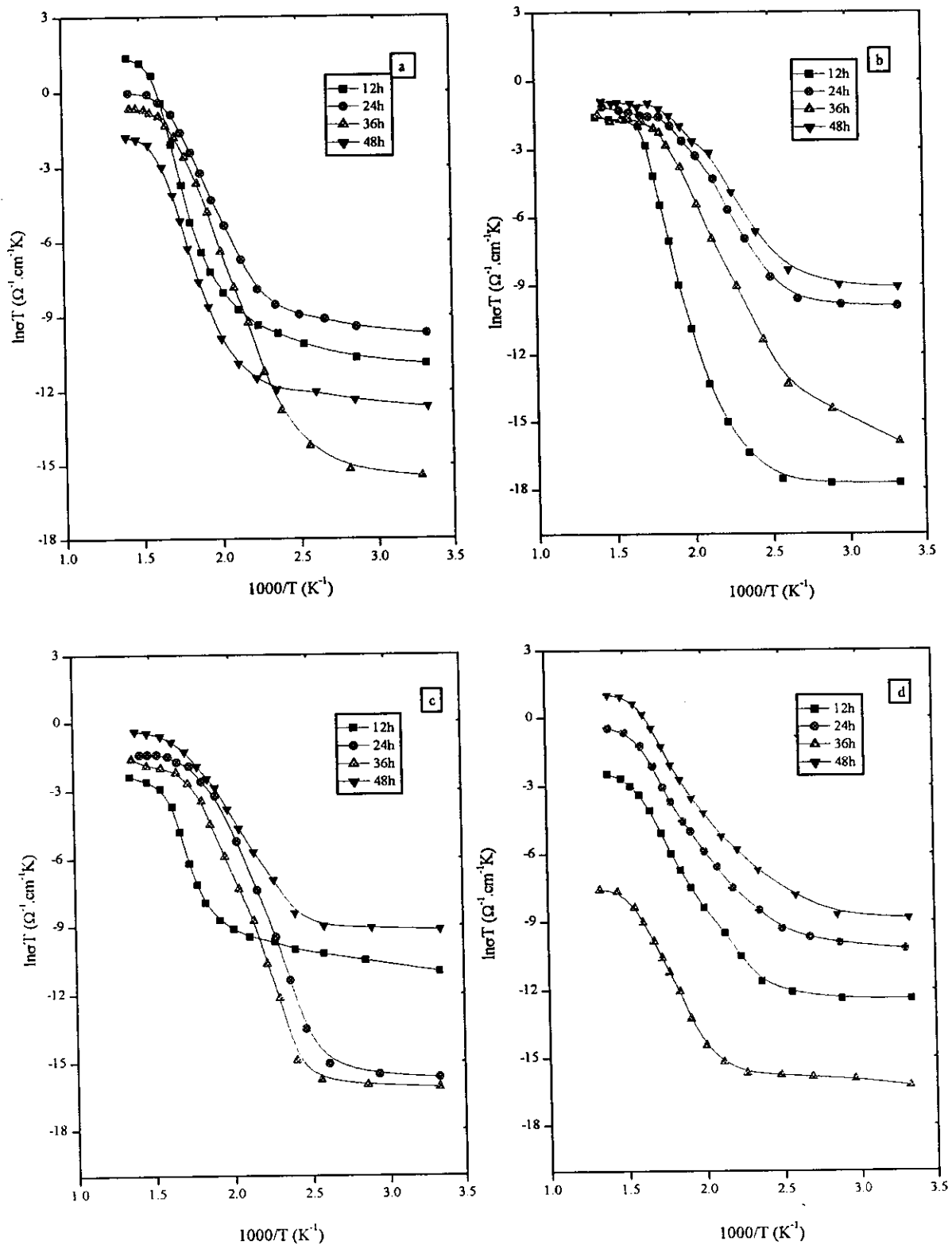


Fig.(3.2:a-d): D.C Conductivity dependence on the reciprocal of absolute temperature after ion exchange for a:(S1), b:(S2), c:(S3) and d:(S4)



The effect of ion exchange on the DC conductivity of the samples is attained by comparing the Figs. (3.1, 3.2). It is clear that the conductivity after ion exchange is slightly better than that before ion exchange. This result is accepted due to present of two silver ions moving together under the influence of an applied electric field to participate in the conduction processes<sup>(31)</sup>.

Also, the inflection points of the conductivity depend on the time of ion exchange of the glasses - referring to the microphase structure that may be contained in the samples. Generally by comparing the breaking points over a wide range of temperature, we can observe that the transition points are deviated into low temperature with increasing the time of ion exchange otherwise the transition points are changed randomly by increasing the sodium contents due to the exchanged deficient silver layer formed in the sample and the host of sodium ions.

Table (3.2): The activation energy as calculated from the D.C conductivity, at low ( $E_{\sigma 1}$ ), high ( $E_{\sigma 2}$ ) temperatures and the inflection temperature (I.T) for the samples S1, S2, S3 and S4 after ion exchange.

Time of exchange	$E_{\sigma 1}$ eV	$E_{\sigma 2}$ eV	(I , T) K	$E_{\sigma 1}$ eV	$E_{\sigma 2}$ eV	(I . T) K
(h)	S1			S3		
12	0.52	1.23	500	0.34	1.10	526
24	0.23	0.94	444	0.22	0.77	400
36	0.27	1.11	435	0.12	0.59	406
48	0.30	1.09	454	0.19	0.79	393
(h)	S2			S4		
12	0.51	1.10	434	0.23	0.99	455
24	0.29	0.83	400	0.19	0.68	434
36	0.31	0.78	392	0.17	0.48	467
48	0.25	0.87	278	0.16	0.65	400

### 3.1.2 AC Conductivity and Dielectric Properties

#### 3.1.2a The Temperature and Frequency Dependence of AC Conductivity

The correlation between conductivity and reciprocal of absolute temperature (350-900) K at different frequencies (100kHz – 2MHz) for the investigated samples  $X(\text{Na}_2\text{O}) \cdot 0.53(\text{SiO}_2) \cdot 0.08(\text{Bi}_2\text{O}_3) \cdot (0.39-X)(\text{B}_2\text{O}_3)$ ;  $X = 0.05(\text{S1}), 0.15(\text{S2}), 0.25(\text{S3})$  and  $0.35(\text{S4})$ , is shown in Fig. (3.3:a-d). The data show that at low temperature region the conductivity  $\sigma_{ac}$  is temperature independent and increases with

increasing frequency for different compositions of the glassy samples. This is interpreted as the frequency acts as a pumping force pushing the charge carriers between the different conduction states, after that in the high temperature region the conductivity is frequency independent, but is largely increasing with increasing temperature. In other words, two straight lines are obtained indicating the different conduction mechanisms. The general trend of the data obeys the well known "Arrhenius" relation <sup>(72)</sup> for ionic diffusion

$$\sigma_{\text{Tot}}T = \sigma' \exp (-E_{\text{ac}} / kT) \quad (3-2)$$

where ( $\sigma'$ ) is a pre-exponential constant, ( $k$ ) is Boltzmann constant, ( $T$ ) is the absolute temperature and ( $E_{\text{ac}}$ ) is the activation energy which is sufficient to activate the charge carriers to participate in the conduction processes. The values of the activation energy are reported in table (3.3).

The Ac conductivity of samples S1 and S2 have nearly the same trend with temperature, giving rise to two distinct regions of conduction. The first one, in the low temperature region the conductivity  $\sigma_{\text{ac}}$  is frequency dependent and temperature independent. The plateau region in the conductivity data near room temperature indicates the metallic like behavior of the samples. In the second region the conductivity becomes strongly dependent on the temperature, where its variation with frequency becomes small; this was assigned as the frequency independent part. The semi-conducting behavior can be demonstrated at high temperature region due to the sharing of sodium ions liberated at this temperature.

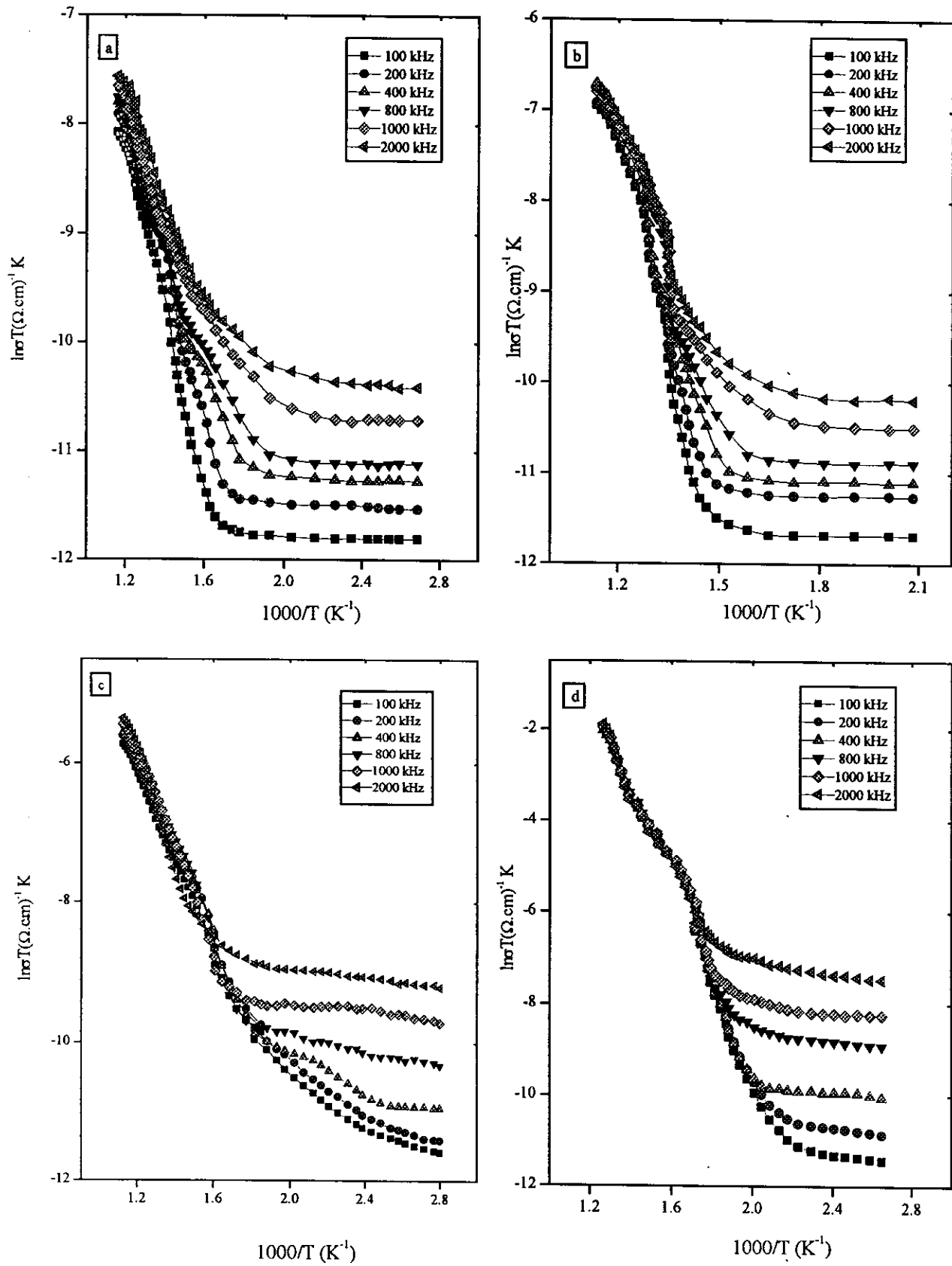


Fig. (3.3:a-d): Relation between conductivity  $\ln\sigma T$  and reciprocal of absolute temperature as a function of the applied frequency for samples a:(S1), b:(S2), c:(S3) and d:(S4)

The reported data shows that samples S3 and S4 behave as a semi conducting material due to their low activation energy. More than one conduction state can be considered for the samples. In the first temperature region, the conduction is mainly electronic which is very clear from the stationary change of the conductivity while with increasing temperature the thermal energy becomes high enough to help in moving ions between the conduction states to participate in the conduction process. In other where, the high thermal energy given to the samples in this region helps in decreasing the internal viscosity though a chance given to ions to move smoothly from one part to another inside the sample. These two processes of conduction were reflected in the dielectric properties where both conductivities and polarization are of the same origin.

Table (3.3): The activation energy (eV) for the different samples at different investigated frequencies at high temperature region

Samples	100 kHz	200 kHz	400 kHz	800 kHz	1000 kHz	2000 kHz
S1	0.90	0.89	0.88	0.87	0.84	0.81
S2	0.72	0.68	0.65	0.61	0.60	0.56
S3	0.59	0.56	0.54	0.50	0.49	0.46
S4	0.53	0.51	0.49	0.47	0.44	0.40

In general, the conduction mechanism in the low temperature range is affected by the formation of electron – ion pairs between the filled and empty states with the boron anomalous behavior site <sup>(51)</sup> and

the framework of the bismuth domains <sup>(31)</sup> in the glasses. While, the conduction at relatively high temperature range is dominated by the hopping of the relatively free Na<sup>+</sup> ions.

From a closer look of all the investigated samples with different sodium oxide concentration, it is obvious that the values of conductivity are increased with increasing sodium concentration achieved with the enhancement of Na<sup>+</sup> ions by sharing in the conductance.

### 3.1.2b The frequency dependence of the total conductivity

The variation of the total conductivity,  $\sigma(\omega)$ , as a function of frequency range (100-2000 kHz) for the investigated glassy system, was studied at different temperatures 350-450-500-550-600-700-800 K and is shown in Fig. (3.4). The feature to note is that the conductivity is shifted up with increasing the temperature. In low temperature range the conductivity increases with increasing frequency up to a certain temperature at which  $\sigma_{\text{tot}}(\omega)$  reaches its small stationary region appears. While in the higher temperature range,  $\sigma_{\text{tot}}(\omega)$  depends on the composition and measured temperature range which varies for each sample.

The variation of  $\sigma(\omega)$  with frequency could be expressed by the following Jonscher's relations <sup>(34)</sup>

$$\sigma_{\text{tot}}(\omega) = \sigma_{\text{dc}} + \sigma_{\text{ac}}(\omega) \quad (3-3)$$

where,  $\sigma_{\text{dc}}$  is the dc conductivity, and  $\sigma_{\text{ac}}(\omega)$  is the polarization conductivity, which can be written as <sup>(96)</sup>

$$\sigma_{\text{ac}}(\omega) = A \omega^s \quad (3-4)$$

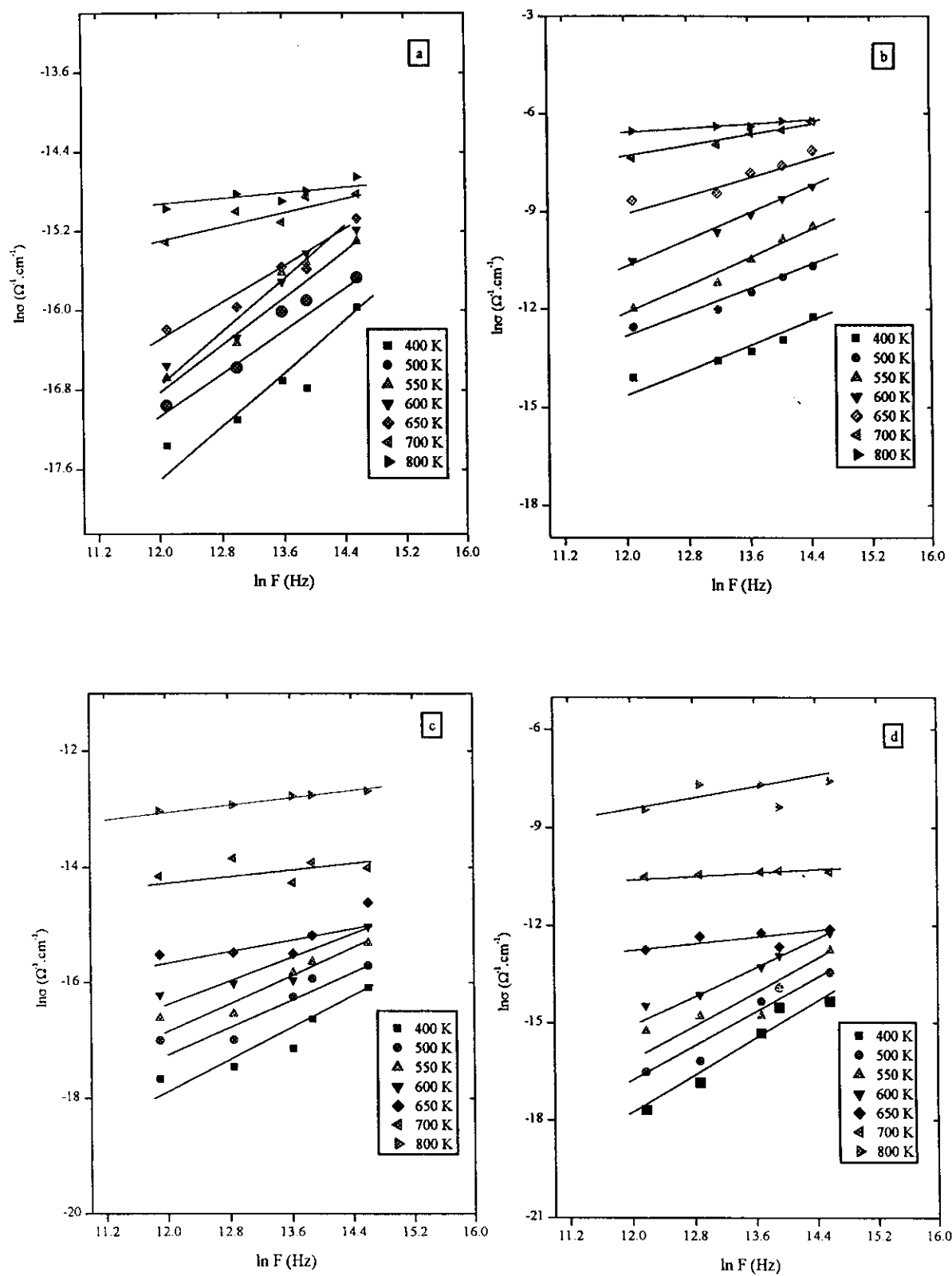


Fig. (3.4): Dependence of conductivity on the frequency at different temperature for the samples a:(S1), b:(S2), c:(S3) and d:(S4).

where A and S, are temperature dependent parameters, and  $\omega$  is the angular frequency. The values of the exponent s are deduced and lie in the range (0.15 - 0.9).

The behavior of s (T) can be taken as a criterion for the conduction mechanism <sup>(95)</sup>. The classical barrier model, for single electron hopping between localized states over a potential barrier separating the sites as well as the correlated barrier hopping model, is suggested for congruent with samples S2 and S3 for the all range of temperature. In the case of sample S1 the small polaron model, is suggested in the low temperature region up to 500 K and the correlated barrier hopping model in the high temperature region. Finally, the large overlapping polaron is suggested for sample S4 in the low temperature region up to 650 K, and the correlated barrier-hopping model is the congruent mechanism in the high temperature region.

### 3.1.2c The temperature dependence on the mean drift mobility

The dependence of the drift mobility  $\mu$  on the absolute temperature as a function of the applied frequency <sup>(96)</sup> is shown in Fig. (3.5).

$$\mu = (\sigma) / (n \cdot e) \quad \text{-----} \quad (3-5)$$

where ( $\sigma$ ) is the temperature dependent conductivity, (e) electron charge and (n) is the number of charge carriers per unit volume;  $n = (N_A \times D) / (M)$ ;  $N_A$  is Avogadro's number, D is the density of glassy samples and M is the molecular weight. In the first temperature region a stable behavior is obtained for  $\mu$  with increasing temperature up to nearly (560, 450, 600, 700 K) for the samples S1, S2, S3 and S4 respectively as nearly congruent with  $T_{cr}$  value of the DSC charts. After that the mobility  $\mu$  increase rapidly with the increasing temperature, which is ascribed to



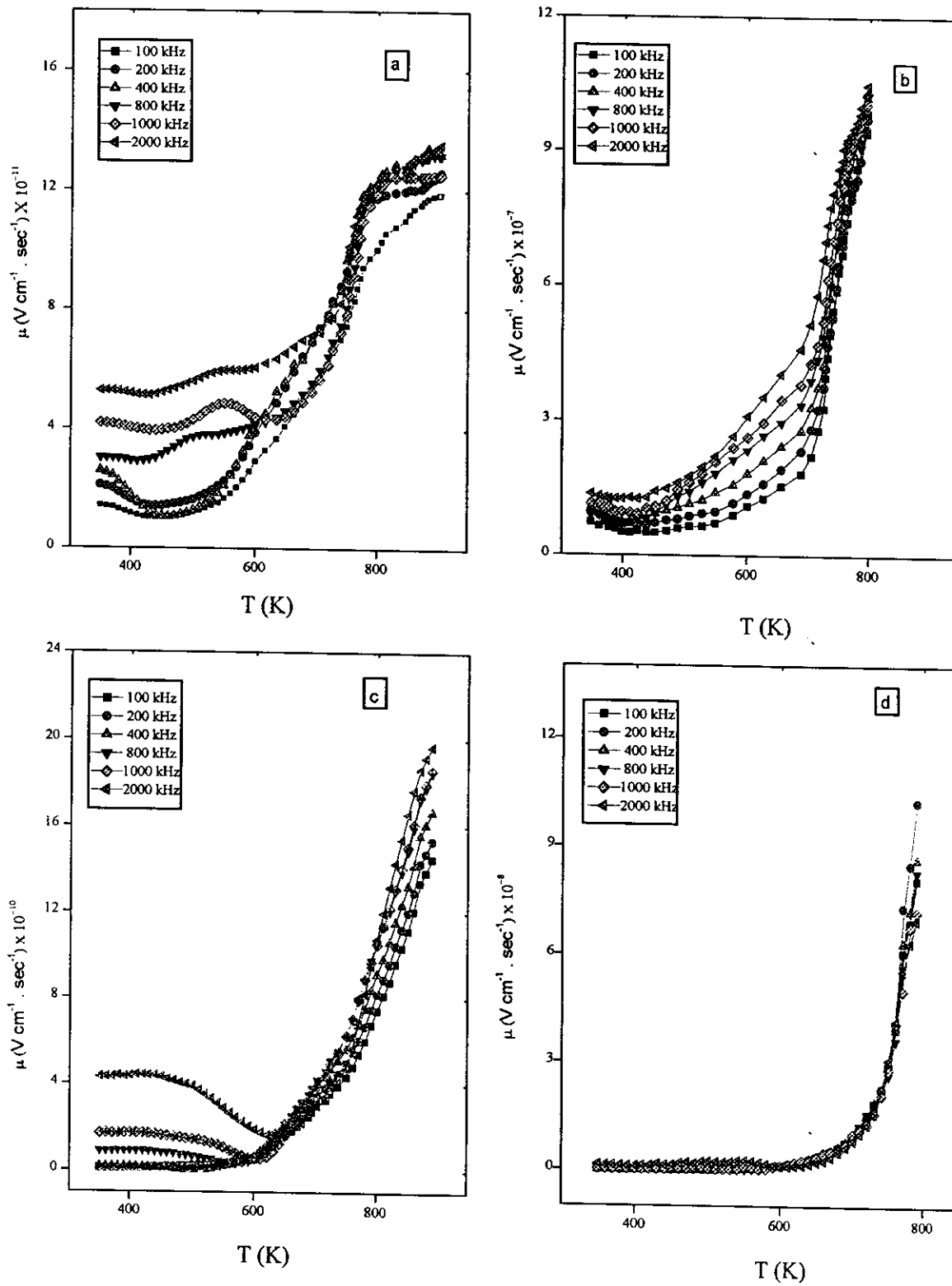


Fig (3.5:a-d): Relation between drift mobility  $\mu$  and absolute temperature as a function of frequency, where a = S1, b = S2, c = S3 and d = S4

the thermal liberation of charge carriers with sufficient energy to share in the conduction mechanism. The increase in the mobility of the samples behave as monotonically change.

The effect of frequency on the mobility values at low temperature region that  $\mu$  is increasing with increasing frequency which can ascribed to the electronic conduction, i.e. the frequency acts as a pumping force helping the electrons to jump from one state to another by considering the range of the frequencies used as low frequency range. The variation of the drift mobility with temperature enhances the use of hopping model of conductivity in the samples, where the charge carrier what ever its type can hop from one conduction state to another.

### **3.1.2d The Temperature and Frequency Dependence of the Dielectric Properties**

#### **(I) Temperature dependence on the dielectric constant**

Figure (3.6) correlates the real part of the dielectric constant  $\epsilon'$  versus absolute temperature  $T$  for the samples S1, S2, S3, and S4 in the temperature range from 350 K up to 900 K as a function of the applied frequency ranged from 100 kHz to 2000 kHz. From the figure it is clear that, S1 has three distinguished regions, the first one (350 – 600) K, in which  $\epsilon'$  is nearly constant with temperature but slightly varies with frequency. This behavior can be ascribed to the partially electronic polarization, which plays a significant role in this region. In the second region (600 – 750) K a slightly increase of the dielectric constant with increasing temperature while the frequency has an influence at this region with a slight hump which depends on both frequency and

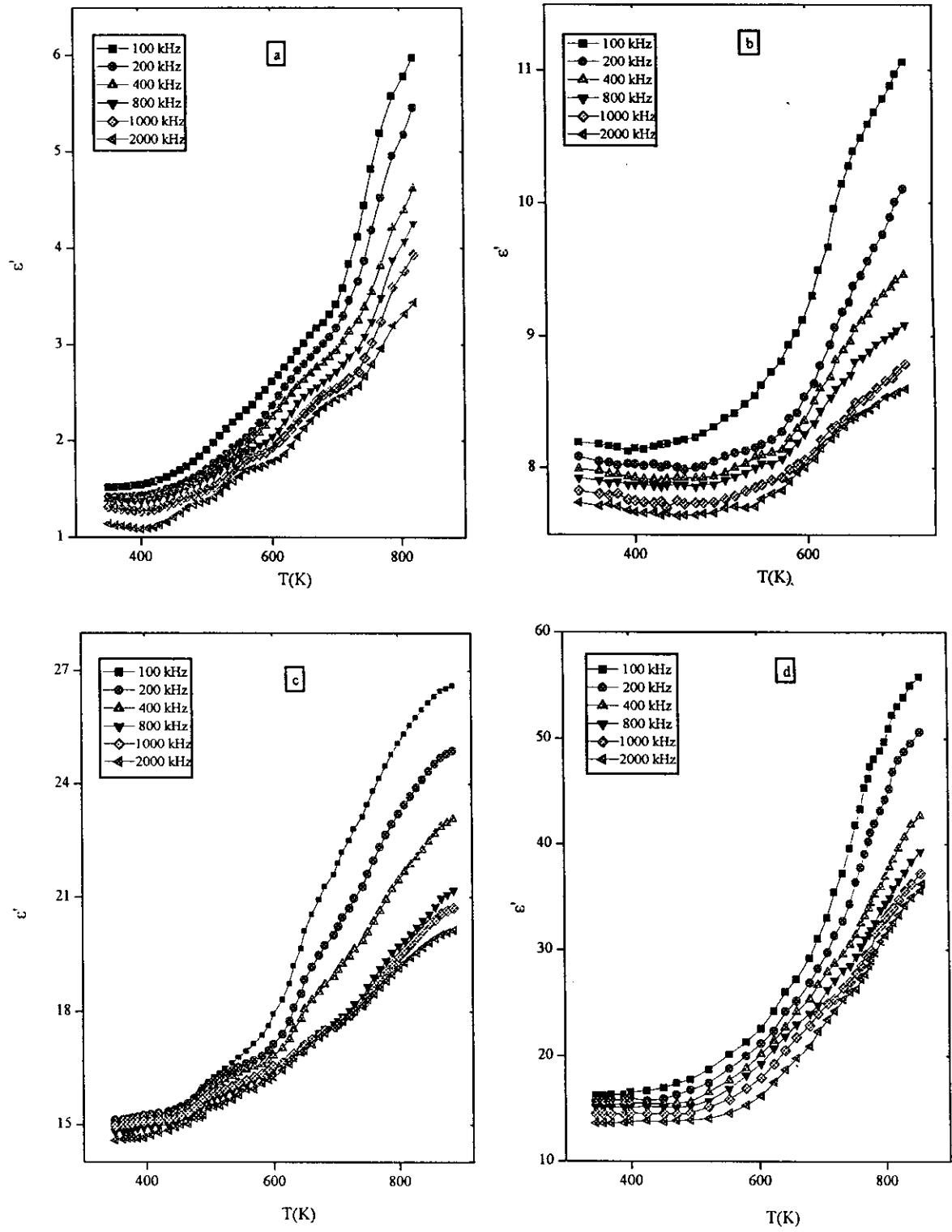


Fig. (3.6:a-d): Dependence of dielectric constant ( $\epsilon'$ ) on the absolute temperature as a function of the applied frequency for the samples a:(S1), b:(S2), c:(S3) and d:(S4)

temperature. This was attributed to the ionic polarization that begins to play a role in cooperation with the electronic one. In the last region,  $\epsilon'$  is largely increased with increasing temperature, which leads to expect that an interfacial polarization take place in addition to the prior polarization. The participation of more than one type of polarization leads to the sudden increase in  $\epsilon'$  with temperature.

Fig. (3.6b) of sample S2 shows two different regions. The first one (350 – 500) K at this region,  $\epsilon'$  have stable values with increasing temperature and the frequency has no effect in this region to mention the participation of electronic polarization. After that in the second region (500 – 750) K a large increase of  $\epsilon'$  was obtained, it is nearly formed due to the participation of ionic and orientational polarization at this region is large affected by the applied frequencies. The thermal energy given to the sample is quite enough to move some of the dipoles (sodium ions) in addition to the electrons, though the ionic polarization participates in the dielectric process, also the interfacial polarization play a predominant role at this region. On the other hand,  $\epsilon'$  decrease with increasing frequency at this region, this may be attributed to equanimity of the field emission of the dipole structure with the applied field.

Fig. (3.6c) represents samples S3, which gives nearly stable state from 350 K up to 550 K after which  $\epsilon'$  gives a continuous increases with increasing temperature giving a small hump at 500 K. More than one transition points were appeared, indicating the presence of more than one polarization mechanism. This could be attributed to the small thermal energy which is insufficient to excite the localized dipoles to be oriented in the field direction, in which the electronic polarization is the most

predominant in this region. After that a large increase of  $\epsilon'$  with increasing the temperature while it decrease with the frequency, this is may be attributed to the existence of some crystalline phases in the glass network, which contributes to the ordering in the sample. After 600K, the participation of interfacial polarization together with the ionic plays a significant role due to embedding of some crystalline phases in the glass matrix. At relatively high temperature, the ionic polarization predominates, as a result of increasing the structure relaxation of glasses by increasing the temperature. The same behavior was obtained for sample S4 but with some variation and small dependence on frequencies at the high temperature region 750 – 850 K.

From a general scope of the data for all samples Fig. (3.6) one can see that, at the relatively low temperature range, the dielectric permittivity is almost temperature independent and after that, it increases with increasing temperature, the rate of the increase is being different with different frequencies. This behavior can be explained on the basis of the presence of inter-microstructure dipoles. Evidently these dipoles remain frozen at lower temperature and by increasing temperature, the glassy network relaxes and the ionic motions become easier and hence  $\epsilon'$  increases with T so the ions have more chance to participate in the motion.

The magnitude of the dispersion of  $\epsilon'$  with frequency was found to increase with increasing sodium content in the samples. This may be attributed to the ability of sodium ion to be polarized to more extent than the bismuth ion in the glass matrix. Also the ionic polarization will participate violently with increasing  $\text{Na}^+$  ions which leads to increase the

sharing of more dipole in the electric conduction given an increase in  $\epsilon'$  value.

## II) Frequency Dependence of the Dielectric constant for the Investigated Glass Samples:

The frequency dependence of the real part of the dielectric permittivity  $\epsilon$  was studied at different ambient temperature with frequencies range 100-2000kHz for the glass system  $[X(\text{Na}_2\text{O}). 0.53(\text{SiO}_2). 0.08(\text{Bi}_2\text{O}_3). (0.39-X)(\text{B}_2\text{O}_3)]$ , where  $X= 0.05(\text{S1}), 0.15(\text{S2}), 0.25(\text{S3})$  and  $0.35(\text{S4})$ . Fig. (3.7:a-d) illustrates that, the frequency dependence of  $\epsilon'$  obeying Debye's equation for the intrinsic relaxation processes. Accordingly,  $\epsilon'$  can be expressed by the following equation <sup>(7)</sup>

$$\epsilon'(\omega) = \epsilon_{\infty} + [(\epsilon_s - \epsilon_{\infty}) / (1 + (\omega^2 \tau^2))] \quad (3-6)$$

where,  $\epsilon_{\infty}$  and  $\epsilon_s$  are the optical and static dielectric constants respectively. Two distinguishable regions are observed. A slight decrease with increasing frequency in the low frequency range followed by a strong dependence on frequency, which was recorded at relatively higher frequencies. The mentioned behavior is shifted upward with increasing temperature for the different concentrations of the samples. This can be attributed to the fact that, at low frequency the dielectric constant  $\epsilon$  is rising by the contribution of both ionic and interfacial polarization <sup>(98)</sup>. When the frequency is raised, the dipoles will no longer be able to rotate sufficiently rapidly so that their oscillations will begin to lag behind those of the field. In addition, the polarization as well as  $\epsilon'$  decrease.

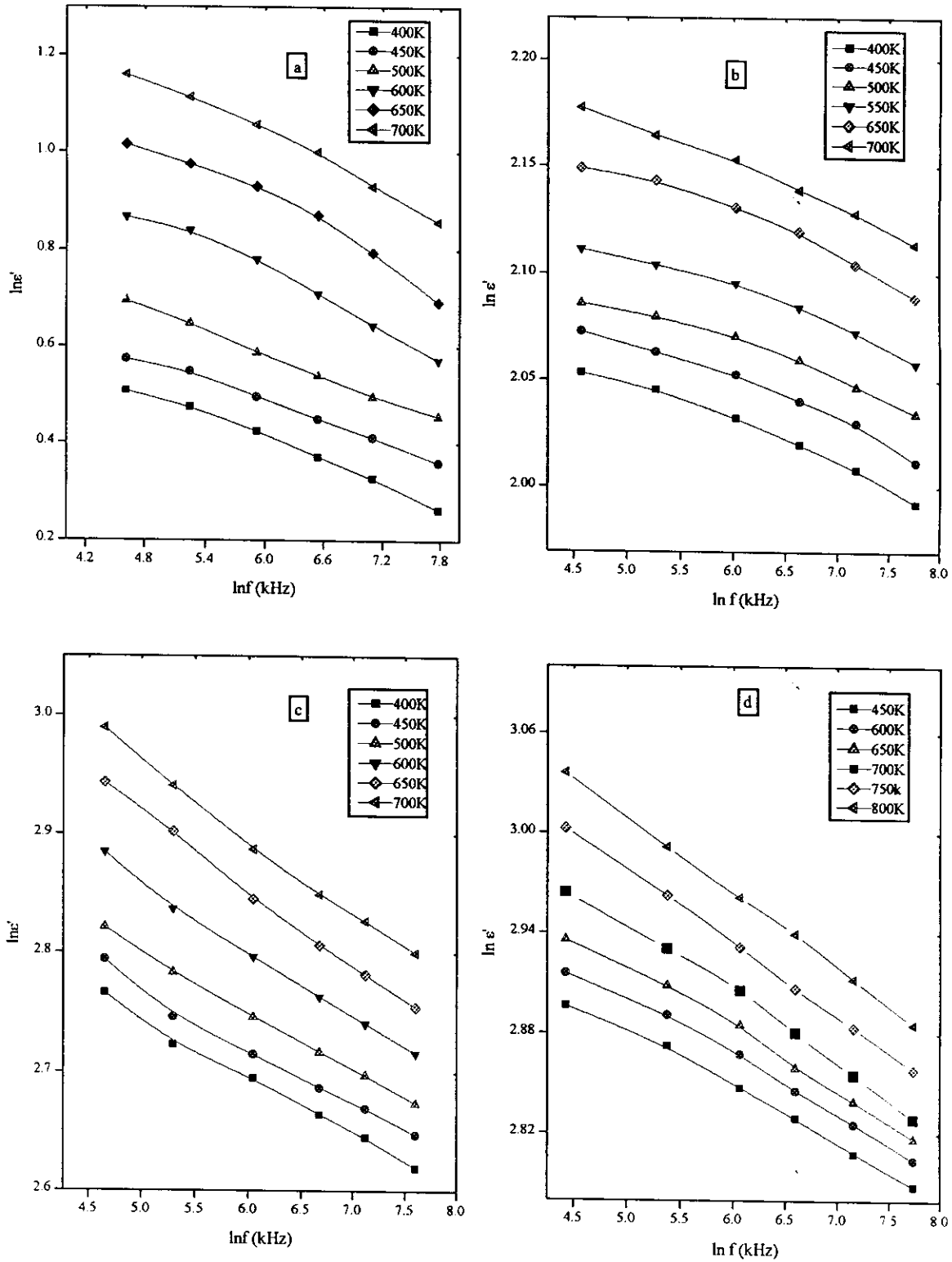


Fig. (3.7:a-d): Dependence of dielectric constant ( $\epsilon'$ ) on the frequency

at different fixed temperature for a:(S1), b:(S2), c:(S3) and (d:S4)

### III) Frequency and Temperature Dependence of the Dielectric Loss:

The frequency dependence of the dielectric loss factor  $\varepsilon''$ , for all the investigated glassy samples is studied at different fixed ambient temperatures. Fig. (3.8a) shows that, the dielectric loss  $\varepsilon''$  decreases as the frequency is increased while a deviation occurs for the case of higher concentration of sodium content. It is also noticed that,  $\varepsilon''$  is shifted upward when the temperature was increased for the glass samples under investigation. The appearance of such mentioned regions depends on the temperature range. Therefore, the frequency dependence of  $\varepsilon''$  could be discussed according to the following relation <sup>(99)</sup>,

$$\varepsilon''(\omega) = (\varepsilon_s - \varepsilon_\infty) 2\pi^2 N (ne^2 / \varepsilon_s)^3 kT \tau_0^m W_M^{-4} \omega^{-m} \quad (3-7)$$

where  $m = -4kT / W_M$

;  $n$  is the number of hopping electrons,  $N$  is the concentration of localized states;  $\varepsilon_s$  is the static dielectric constant and  $\varepsilon_\infty$  is the dielectric constant at high frequencies and  $W_M$  is the energy required to liberate a carrier. Then the relation (3-7) can be reformulated as,

$$\varepsilon''(\omega) = A \omega^{-m} \quad (3-8)$$

The values of the exponent  $m$  are obtained by using the least square fitting of equation (3-8) and listed in Table (3.4). The reported data show that, the value of the exponent  $m$  decreases with increasing temperature.



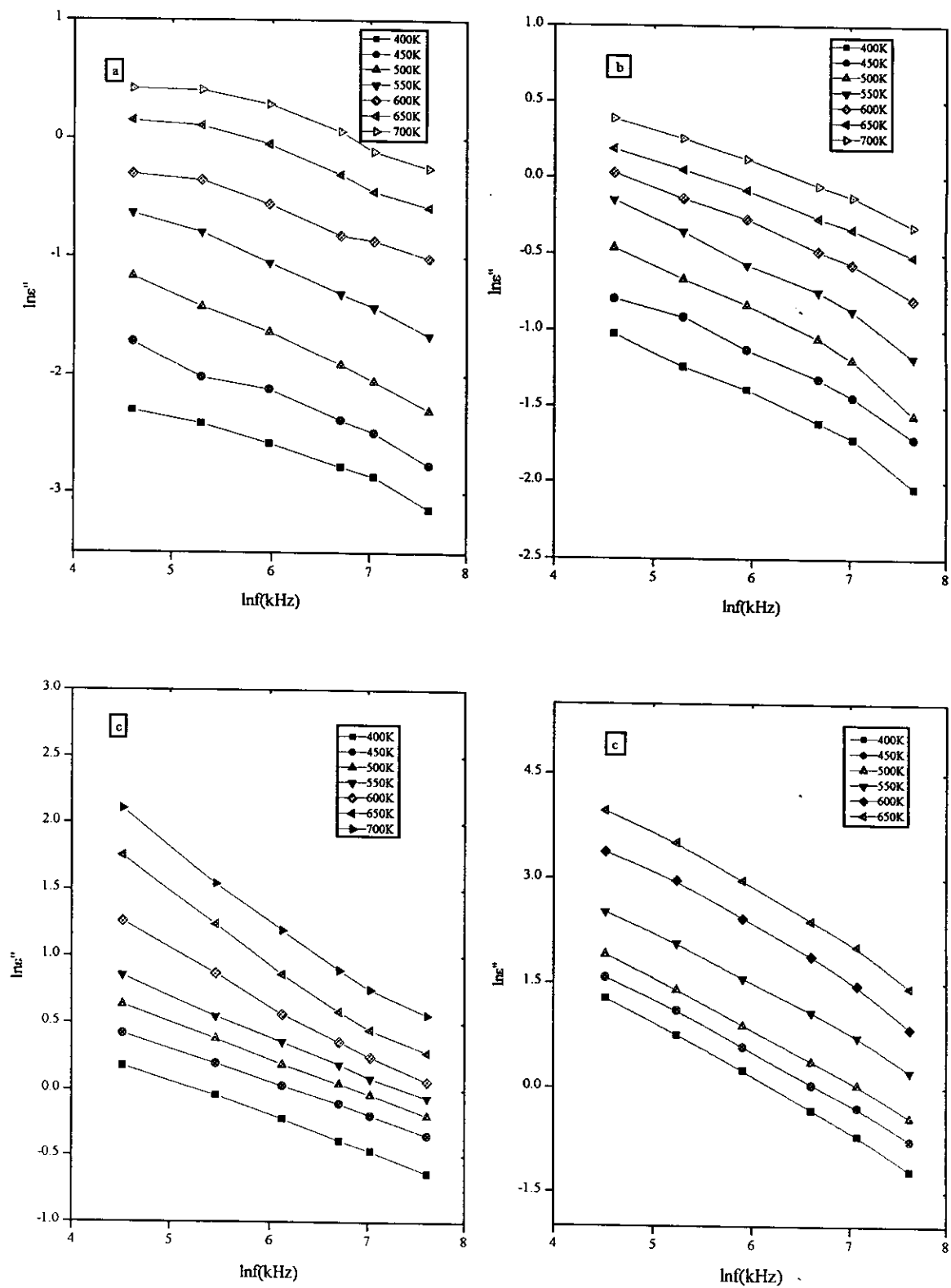


Fig. (3.8:a-d): Dependence of dielectric loss factor ( $\epsilon''$ ) on the frequency

at different temperature for samples, a:S1, b:S2, c:S3 and d:S4

Table (3.4): Values of Exponent (m) of  $[X(\text{Na}_2\text{O}). 0.53(\text{SiO}_2). 0.08(\text{Bi}_2\text{O}_3). (0.39-X)(\text{B}_2\text{O}_3)]$ ; X= S1 (0.05), S2 (0.15), S3 (0.25), S4 (0.35) glass system at different temperature

Temperature (K)	S1	S2	S3	S4
400	0.39	0.29	0.39	0.01
450	-0.64	-0.11	0.22	-0.05
500	0.39	-0.27	0.12	-0.18
550	0.27	-0.32	0.00	-0.21
600	0.41	-0.35	0.00	-0.23
650	0.34	-0.47	-0.03	-0.20
700	0.38	-0.49	-0.07	-0.17
750	-0.32	-0.52	-0.93	-0.69
800	0.32	-0.62	-0.85	-0.63

The values of  $W_M$  are reported in Table (3.5), it is noticed that the values of  $W_M$  increase with increasing the concentration of  $\text{Na}_2\text{O}$ . This may be attributed to the structure rigidity and less doorways for the glassy systems. The obtained values of the barrier height  $W_M$  seem to be larger than  $kT$ , which predicts the diffusion of Na ions to participate in the conduction mechanism.

Table (3.5): The obtained values of the liberating Energy ( $W_m$ ) (eV) of the glass system at different temperature

Temperature (K)	S1	S2	S3	S4
400	-5.62E-20	-7.69E-20	-5.73E-20	-2.10E-18
450	3.86E-20	2.20E-19	-1.14E-19	4.61E-19
500	-7.05E-20	1.02E-19	-2.33E-19	1.51E-19
550	-1.11E-19	9.37E-20	-2.53E-17	1.45E-19
600	-8.00E-20	1.33E-19	1.84E-17	1.43E-19
650	-1.05E-19	7.68E-20	1.08E-18	1.81E-19
700	-1.02E-19	9.34E-20	5.44E-19	2.32E-19
750	1.28E-19	4.17E-20	4.47E-20	6.00E-20
800	-1.36E-19	7.15E-20	5.20E-20	6.98E-20

The frequency dependence of the dielectric loss factor  $\epsilon''$ , can be attributed to the diffusion of sodium ions ( $Na^+$ ) in glassy samples, which reduces with increasing frequency. From another point of view, if an alternating electric field is applied for the glass samples, the dipoles can follow the change of the field direction only if the pairs can reorient quickly enough. Since the reorientation involves the jumping of charges into the vacancies, they can only follow alternating field of frequency ( $f$ ) less than the jump rate ( $p$ ). For  $f > p$  the pairs do not contribute to the relaxation permittivity. When the frequency is nearly equal to the rate  $p$ , there is a phase lag between the applied field and the polarization of the glass, and the energy absorbed reaches its optimum value. For all samples the mentioned range of temperature and frequency show dispersion in  $\epsilon''$  which, suggest that the ionic relaxation decreases with

increasing frequency. The ionic relaxation may depend on the activation energy required for crossing the barriers.

Figure (3.9:a-d), shows the temperature dependence of  $\epsilon''$ , at various frequencies for the glass systems  $[X (\text{Na}_2\text{O}). 0.53 (\text{SiO}_2). 0.08 (\text{Bi}_2\text{O}_3). (0.39-X) (\text{B}_2\text{O}_3)]$ , where  $X = (0.05, 0.15, 0.25, 0.35)$ . From the figure it is clear that the values of  $\epsilon''$  increase with increasing temperature. In addition, the dielectric loss factor  $\epsilon''$  increases when the concentration is increased. This indicates that the loss is mainly due to the ionic migration. This based on the fact that the increase of concentration means more restriction of ionic orientation. Low concentration leads to a decrease in the movement of ions in the glass network.

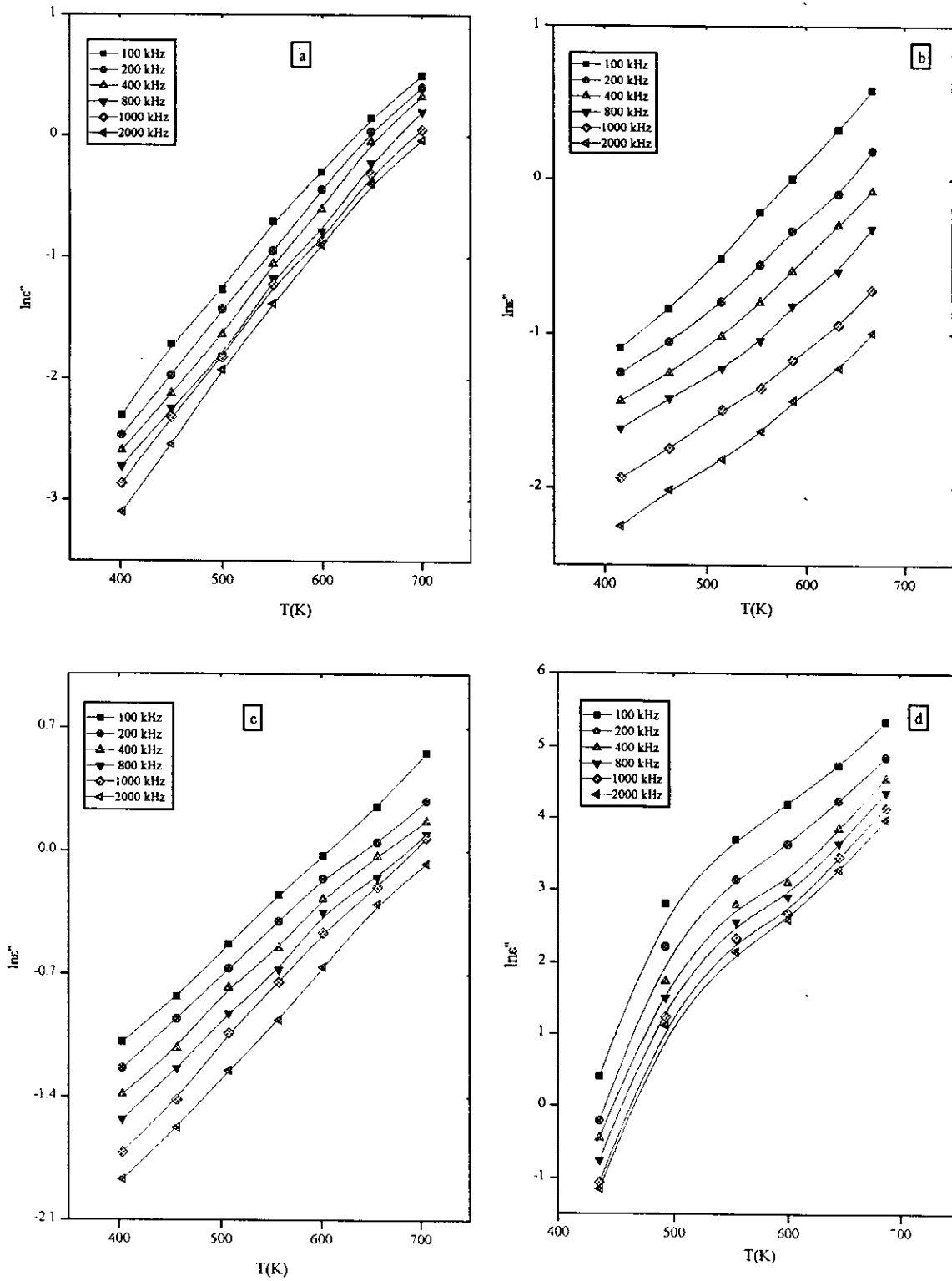


Fig. (3.9:a-d): Dependence of dielectric loss factor ( $\epsilon''$ ) on the absolute temperature at different frequencies for samples a:(S1), b:(S2), c:(S3) and d:(S4)

Table (3.6): The activation energy of the D.C conductivity in the high temperature region ( $E_{dc}$ ) and breaking temperature for the investigated samples

Sample No.	$E_{dc}$ (eV)	Breaking temperature (K)
S3	0.71	588
S5	0.69	525
S6	0.89	650

### 3.2.2 AC Conductivity and Dielectric Properties

#### 3.2.2. a The Temperature and Frequency Dependence of AC Conductivity

The temperature dependence of the A.C conductivity,  $\ln(\sigma_{ac} T)$  at different frequencies 100 – 2000 kHz for the samples  $[0.25X_2O, 0.53SiO_2, 0.14B_2O_3, 0.08Bi_2O_3]$ ;  $X=Na$  (S3),  $Ag$  (S5),  $K$  (S6), was studied from 350 K up to 850 K, and shown in Fig. (3.11). From the figure, it is noticed that, the conductivity values are shifted upwards with increasing frequency and stationary change with increasing temperature i.e. the conductivity is temperature independent at relatively low temperature region, otherwise at high temperature region the conductivity become strongly dependent on the temperature, where its variation with frequency become small, which is assigned as a frequency independent part. The data of conductivity obey the Arrhenius relation for ionic diffusion (3-2).

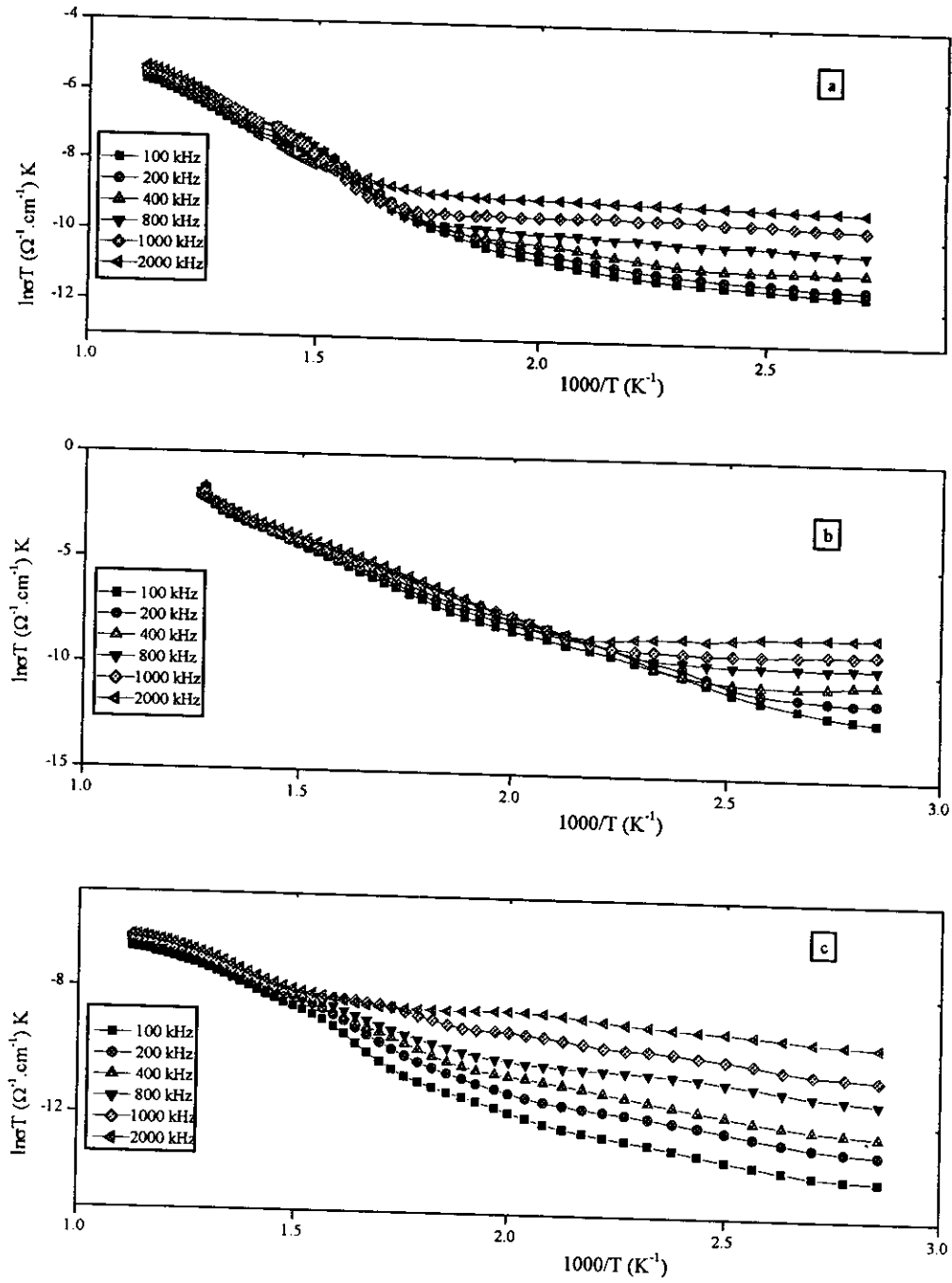


Fig. (3.11:a-c): Dependence of the AC conductivity  $\ln\sigma T$  on the reciprocal of temperature at different frequencies for a:(S3), b:(S5), c:(S6)

The activation energy in the high temperature region is calculated and listed in Table (3.7).

The reported values of the activation energy reveal the semiconducting behavior <sup>(100)</sup> of the investigated samples. One of the important observations of rising conductivity with the applied frequency at low temperature region, that the applied frequency acts as a pumping force for the charge carriers, (electrons and/or ions) between the different localized states of the occupant and empty states to contribute in the conduction process <sup>(35)</sup> i.e. the applied frequency affects on the mobility of the charge carriers as well as their conductivity.

The variation of the conductivity at three different temperatures 400, 500, 666 K at definite frequency 800 kHz for the different alkali metal oxides (S3- S5- S6) is deduced and listed in table (3.8).

From the table, it is clear that the A.C conductivity, at high temperature (666 K), for sample S5 is higher than samples S3 and S6 otherwise the conductivity of S3 and S5 are higher than sample S6 in the low temperature region (400K).

From the data in table (3.8) it can also be observed that the values of the conductivity for all the samples (S3, S5 and S6) at (666K) are higher than those at (400K).



### 3.2.2.b The Frequency Dependence of the Total Conductivity

The variation of the total conductivity,  $\sigma_{\text{Total}}(\omega)$ , is studied as a function of frequency in the range 100-2000 kHz, for the investigated glassy samples with different ambient temperatures 350-450-500-570-660-710-750-800 K. The variation of  $\sigma_{\text{Tot}}(\omega)$  with frequency could be expressed according to the relation (3-3 and 3-4).

The variation of AC conductivity against frequency at different temperatures is shown in Fig. (3.12: a-c). From the figure it is noticed that, the conductivity values are shifted up towards higher values of the temperature depending on the type of the alkali metal oxide and on the measured temperature range. At low temperature, the conductivity increases with increasing frequency except for sample S5 that has a slight and definite raise with increasing temperature. The strongly dependence of conductivity on frequency may be attributed to the minimum heterogeneity in the glasses which reduces the interfacial polarization effects.

As the ambient temperature is increased at higher range, a stationary region of frequency appears that depends on the temperature range, which is characterized by a frequency independent conductivity.

The conductivity is proportional to  $\omega^s$ , where (s) has a value depending on the heat treatment of the sample and lies in the range of (0.15 – 0.88). The conduction mechanism is affected by the formation of ion transfer <sup>(51)</sup>, and the conduction at relatively high temperature dominates by the hopping of the relatively free ions, which obeys the interchange transport model <sup>(108)</sup>. In addition, the correlated barrier model

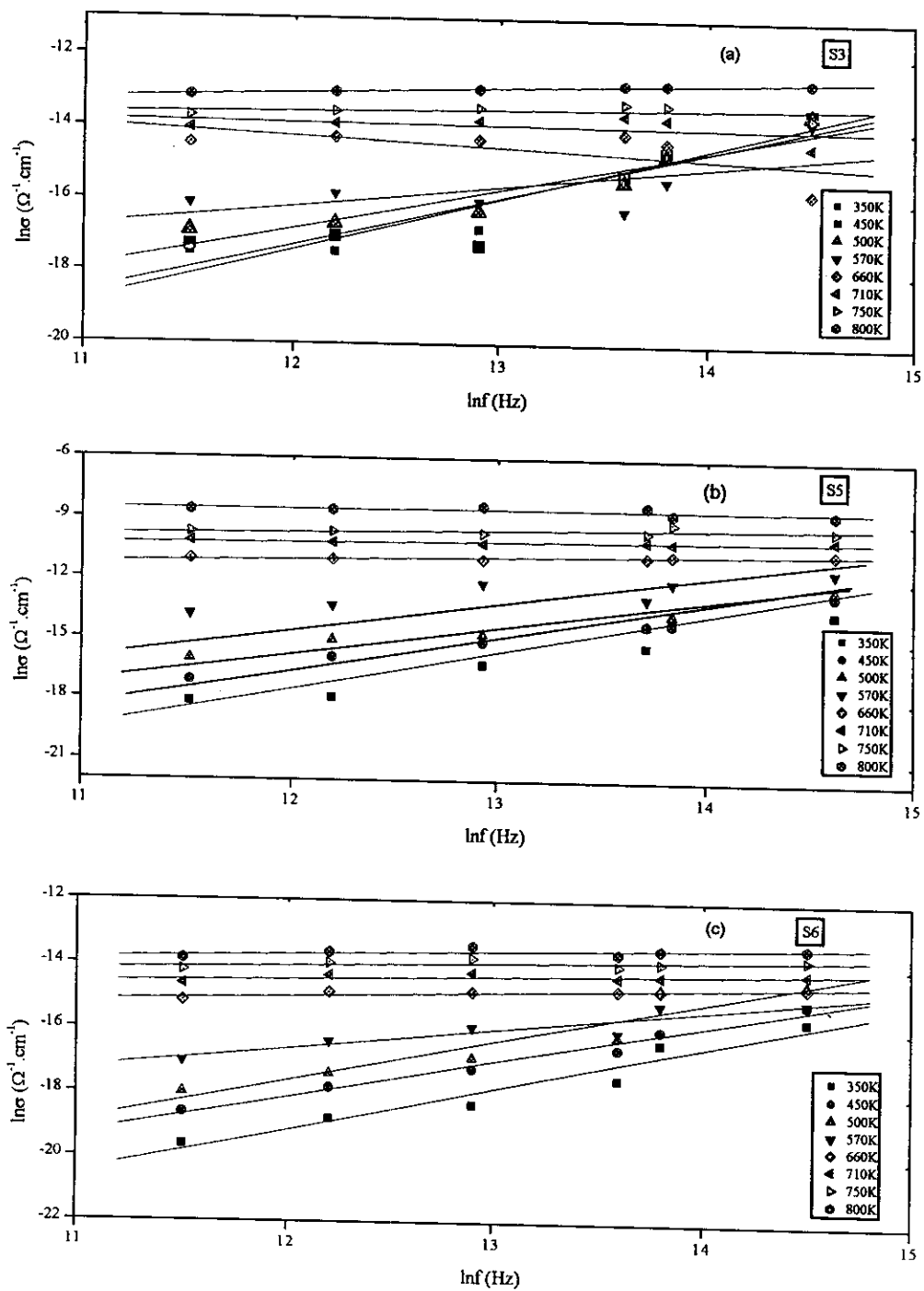


Fig. (3.12:a-c): Dependence of the AC conductivity on the frequency at different fixed temperatures for a:(S3), b:(S5) and c:(S6).

<sup>(95)</sup> is the predominant mechanism observed over all the temperature range.

### **3.2.2.c The temperature dependence on the mean drift mobility**

Figure (3.13a-c) correlates the drift mobility ( $\mu$ ) and absolute temperature for the investigated samples, according to the relation (3-5). The data clarify that, three main regions are obtained. The first one is the nearly stable region, which extends from 350K to about 620K. In this region, the drift mobility is nearly constant with increasing temperature and shifted up with increasing frequency except for sample S5, in the second region, there is a slight increase of  $\mu$  with increase temperature and narrow band dependence of frequencies. The third region in which there is a drastic change of  $\mu$  with both temperature and frequency occurs. This means that in the first region the drift mobility has no detectable variation due to thermally generation of charge carriers and can be ascribed as metallic like behavior. In the second and third regions, it is observed that the mobility increases with increasing temperature, so the variation of the mobility with temperature and frequency enhances the use of hopping model of conductivity where the charge carriers can jump from one place to another in the sample. This indicates that the increase in the drift mobility of the samples under investigation is due to thermally activated mobility, and not to thermally activated creation of charge carriers. It could be noticed that the frequency affects on the mobility of the charge carriers as well as their conductivity.

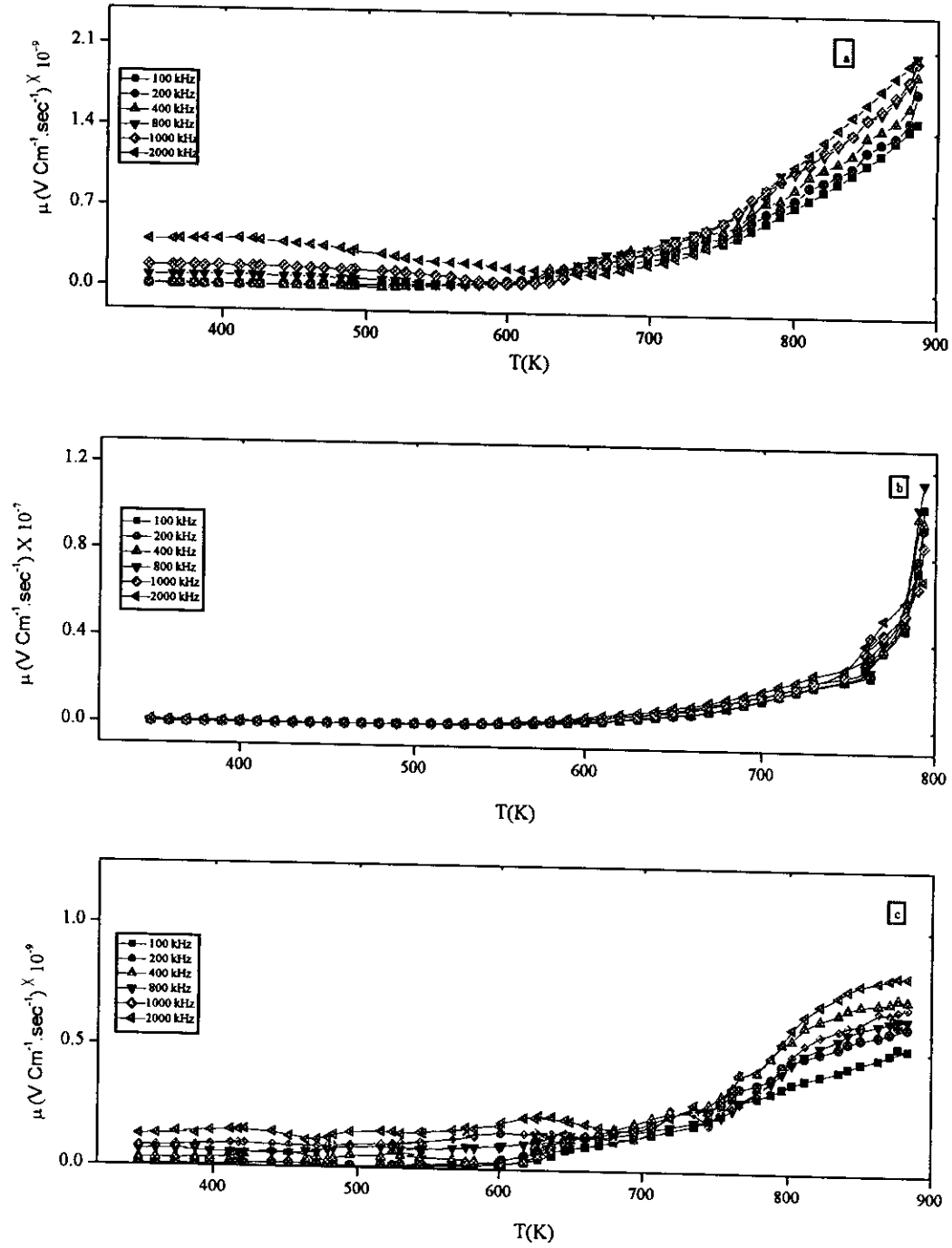


Fig (3.13:a-c): Relation between drift mobility and absolute temperature as a function of frequency for a:(S3), b:(S5) and c:(S6)

### 3.2.2.d The Temperature Dependence of the Electric Dipole Moment

Figure (3.14:a-c) indicates the variations of the electric dipole moment  $\mu'$ , with the absolute temperature. For the samples  $[0.25X_2O, 0.53SiO_2, 0.14B_2O_3, 0.08Bi_2O_3]$ ;  $X = Na$  (S3),  $Ag$  (S5),  $K$  (S6); From the figure it is clear that there are two different regions; at the first region that from 350K to 560K, the dependence of the dipole moment on the temperature is increasing while independent on the frequency. In the second region (above 560K) there is a slight increase of the dipole moment with increasing temperature but the frequency begins to affect on the behavior which produces an increase in the dipole moment with increasing frequency. Sample S6 attained a different behavior of  $\mu'$  which given a stationary increase with increasing temperature up to 580K, after that a drastic decrease of  $\mu'$  with increasing temperature is obtained as calculated <sup>(104)</sup> from the relation

$$\mu' = \sqrt{kT / N (\chi + \beta)} \quad (3-9)$$

where  $k$ ,  $T$  and  $N$  are the Boltzmann's constant, absolute temperature, and the number of electric dipoles per unit volume ( $N = n / 2$ ) respectively, where, ( $n$ ) is the number of charge carriers per unit volume;  $n = (N_A \times D) / (M)$ , where ( $N_A$ ) is Avogadro's number, ( $D$ ) is the density of glass samples, ( $M$ ) is the molecular weight, ( $\chi$ ) is the electric susceptibility and ( $\beta$ ) is a constant which are :  $\chi = [1 / 4\pi (\epsilon' - 1)]$  and  $\beta = [4\pi / (2\epsilon' + 1)]$ . The data in the figure shows that the dipole moment increases with increasing temperature passing by the glass transition point  $T_g$ . It could be seen that the frequency affects directly on the electric dipole moment but in a reversed manner, in comparison to  $\epsilon'$  data, where the values here increase with increasing frequency.

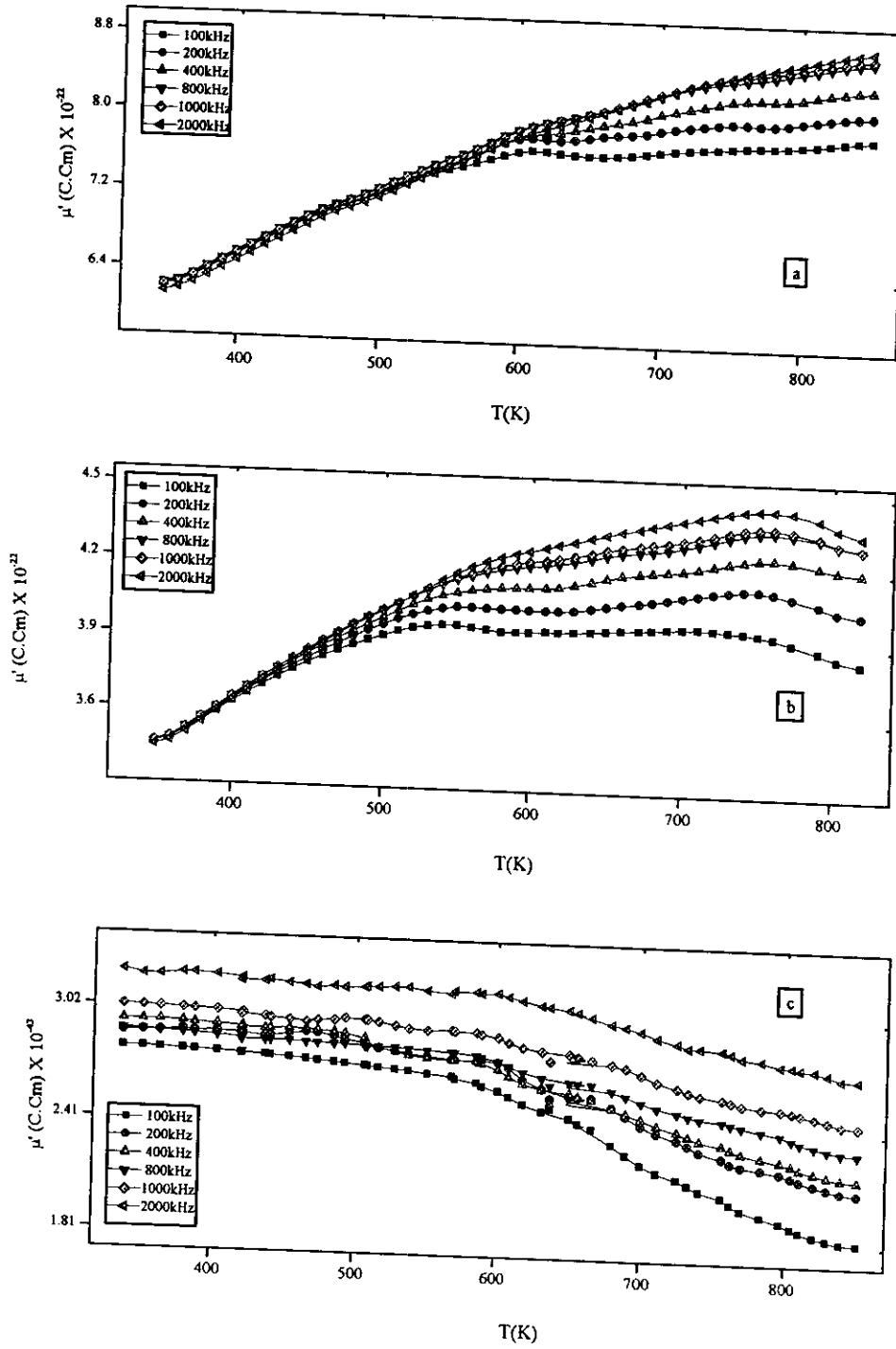


Fig (3.14:a-c): Relation between the electric dipole moment and absolute temperature at different frequencies for a:(S3), b:(S5) and c:(S6)

### 3.2.3 The Temperature and Frequency Dependence of the Dielectric Properties

#### (I) Temperature Dependence of the Dielectric constant

Figure (3.15:a-c) correlates the dielectric constant  $\epsilon'$  against the absolute temperature as a function of different frequencies (100 kHz - 2 MHz), for the investigated glass samples [0.25X<sub>2</sub>O, 0.53SiO<sub>2</sub>, 0.14B<sub>2</sub>O<sub>3</sub>, 0.08Bi<sub>2</sub>O<sub>3</sub>]; X = Na (S3), Ag (S5), K (S6) of 25mol. %. From the graph, it can be noticed that the dielectric constant  $\epsilon'$  is temperature independent, from room temperature up to  $\approx 550$  K, after that  $\epsilon'$  increases with increasing temperature, where its value decreases as the applied frequency increases but with different rates. The variation of  $\epsilon'$  with both temperature and frequency range reveal more than one polarization mechanisms. From a closer look to the data, one can find that the sample S5 have a higher value of  $\epsilon'$  than the samples S3 and S6, that may be attributed to the large number of participating dipole as a result of the larger atomic number of S5 <sup>(47)</sup> rather than that of S3 and S6 <sup>(11,19)</sup> respectively, where  $\epsilon'$  increases by increasing the density of the materials.

The figures have similar trend, which is the common feature of the dielectric materials, as reported by Bahita, et. al.<sup>(102)</sup>. In addition, the behavior of the samples has nearly the same trend. The slight increase of  $\epsilon'$  in the temperature region from room temperature up to nearly 550 K could be attributed to the small thermal energy which is insufficient to excite the localized (frozen) dipoles to be oriented in the field direction, resulting in a small polarizability as well as low value of dielectric constant. This behavior can be ascribed to the participation of interfacial

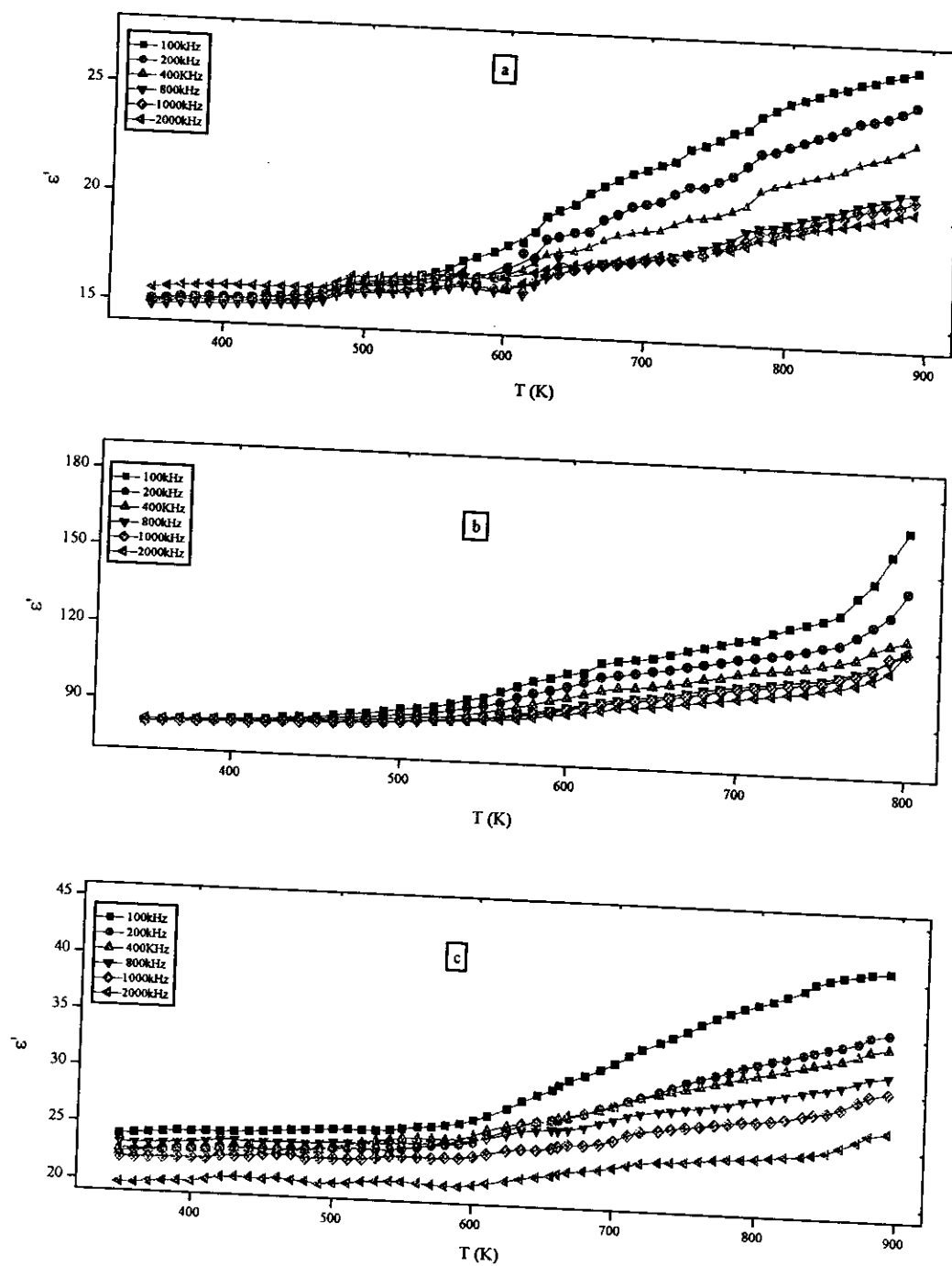


Fig. (3.15:a-c): Temperature Dependence of Dielectric Constant ( $\epsilon'$ ) at different frequencies for a:(S3), b:(S5) and c:(S6).



polarization due to impeding some crystalline phases in the glass matrix besides the ionic polarization. At relatively high temperature (above 550 K), more than one type of polarization such as rotational and orientational polarization of the dipoles were expected <sup>(102)</sup>. This is because the high thermal energy in cooperation with the applied frequency excites more of the frozen dipoles and consequently increases the dielectric constant, in addition to the participation of the ionic polarization, as a result of increasing the structure relaxation of glasses by increasing the temperature; this will facilitate the ionic polarization.

The absence of a maximum in the dependence of the dielectric constant on the temperature for the whole frequency range is an indication of the non-ferroelectric behavior of glass samples. The converse is obtained about nearly 600 K for S3 and S5 that may indicate the existence of some ferroelectricity in the samples due to the presence of a hump as reported in Kittle <sup>(100)</sup> assumptions. The behavior of increasing  $\epsilon'$  with increasing the temperature, and it's decreasing with the frequency, is not a surprising trend as it follows the general behavior of most ionic glasses as reported by R. M. Hill <sup>(104)</sup>.

Generally, the observation of phase separation is one of the important conditions for glass conduction. The presence of these phases is ascribed to a large atomic weight of the compounds which increase the entropy, or for the heterogeneous process of the compound <sup>(100)</sup>, with unsuitable cooling is reached from a single phase region.

The Bismuth ion is one of the essential elements forming the main skeleton of the investigated glasses, it plays a significant role in the polarization processes, since its ionization potential (185 k cal /g. mole)

and sodium ionization potential (119 kcal/g.mole), accordingly at the high temperature region the thermal energy will relax the glassy network, and the ions with low ionization potential such as ( $\text{Na}^+$ ), and ( $\text{Bi}^{3+}$ ), will be able to move easily with the result of increasing  $\epsilon'$  with higher rate <sup>(103)</sup>.

## **(II) Frequency Dependence of the Dielectric constant of the Investigated Glass Samples**

The frequency dependence of the real part of the dielectric constant  $\epsilon'$  was studied at different ambient temperature with frequency ranges 100-2000 kHz for the investigated glassy system. Fig. (3.16:a-c) illustrates that, the frequency dependence of  $\epsilon'$  obeying Debyes equation for the intrinsic relaxation processes  $\epsilon'$  can be expressed according to relation (3.6).

From the figure it is obvious that the values of the dielectric constant are shifted upward with increasing temperature for all the different samples. Otherwise  $\epsilon'$  decreases with increasing frequency at lower frequency followed by a strong dependence on frequency, which was recorded at relatively higher frequencies. This can be attributed to the fact that, at low frequency the dielectric constant  $\epsilon'$  is increased by the contribution of both ionic and interfacial polarization <sup>(98)</sup>. When the frequency is raised, the dipoles will no longer be able to rotate sufficiently rapidly so that their oscillations will begin to lag behind those of the field. Therefore, the polarization will be decreased.

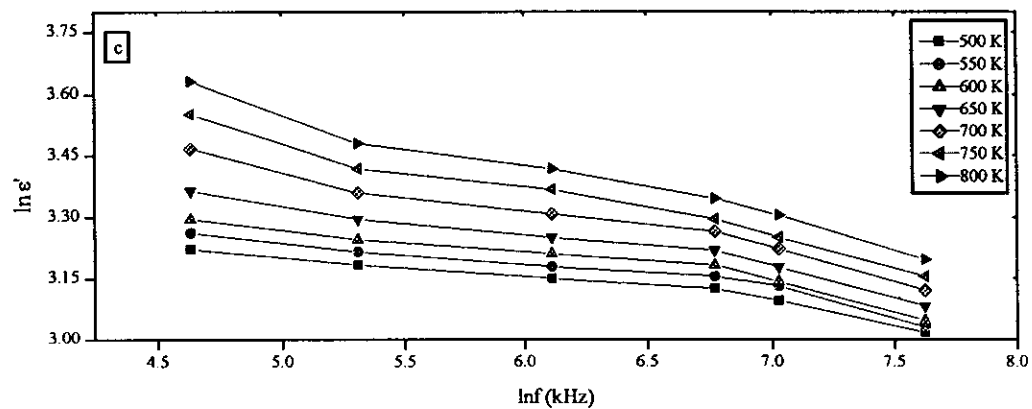
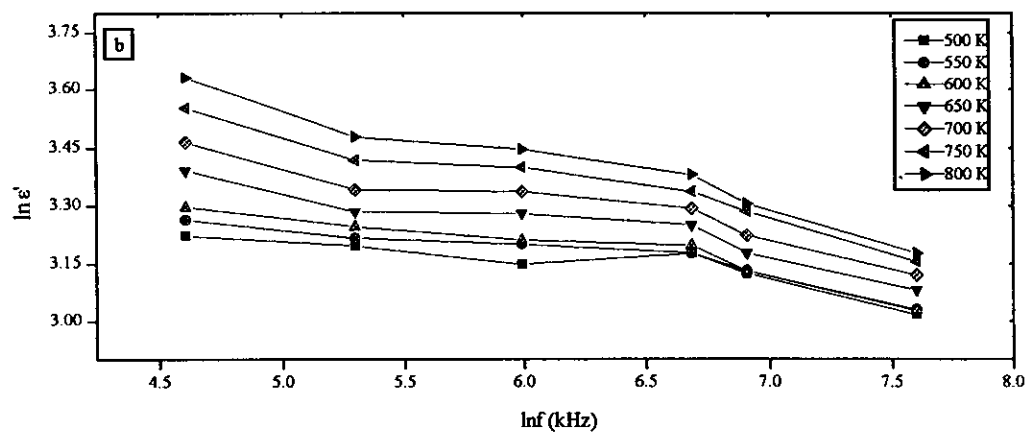
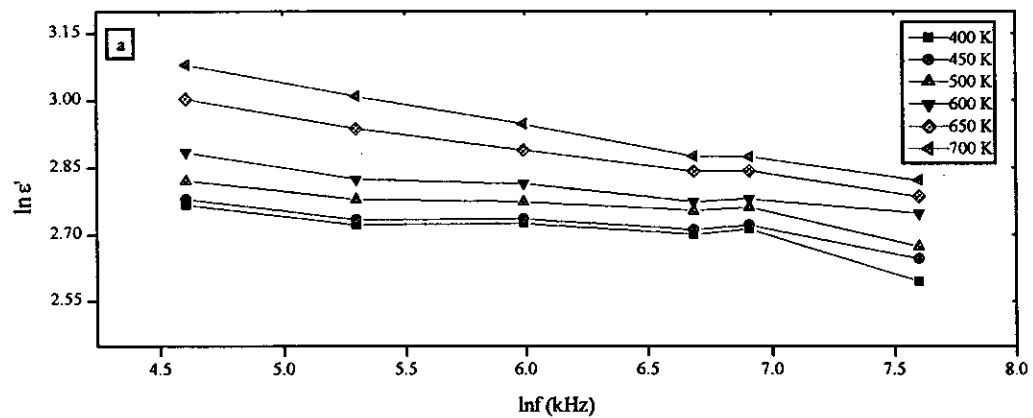


Fig. (3.16:a-c): Frequency dependence of the dielectric constant ( $\epsilon'$ )

at different fixed temperature for a:(S3), b:(S5) and c:(S6).

### (III) The Frequency and Temperature Dependence of the Dielectric loss

The frequency dependence of the dielectric loss factor  $\epsilon''$ , for the glass system  $[0.25(X_2O). 0.53 (SiO_2). 0.08 (Bi_2O_3). 0.14 (B_2O_3)]$ , where  $X = Na (S3), Ag (S5) \text{ and } K (S6)$ , is studied at different fixed ambient temperatures 500, 550, 600, 650, 700, 750, 800 K. Figure. (3.17:a-c) shows that,  $\epsilon''$  is shifted upward when the temperature increases for the glass samples under investigation. It is also noticed that,  $\epsilon''$  decreases slightly as the frequency increases, which varies from one sample to another. Therefore, the frequency dependence of the dielectric loss  $\epsilon''$  could be discussed according to the relations (3-7 and 3-8).

The values of the exponent  $m$  are obtained by using the least square fitting of equation (3-8) for all the samples and listed in table (3.9). It is clear that, the values of the exponent  $m$  for samples S3 and S6 increase with the increase in temperature except for sample S5 is randomly changed with increasing temperature. The values of  $W_m$  are deduced and given in Table (3.10). From the reported data, it is noticed that the values of  $W_m$  vary with the type of the alkali metal oxide, which depend on the inter crystallization structure and the characterization heterogeneity of phases in the samples. The obtained values of the barrier height,  $W_m$  seem to be larger than  $kT$ , which predicts the diffusion of ions to vacancy sites, to participate in the conduction mechanism.

The frequency dependence of the dielectric loss factor  $\epsilon''$ , can be attributed to the diffusion of the ions in the glassy network, which is reduced with increasing frequency.

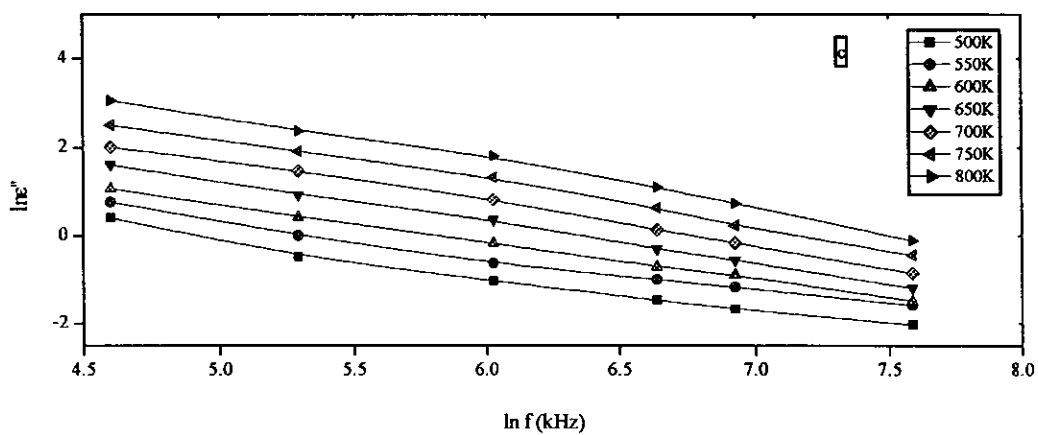
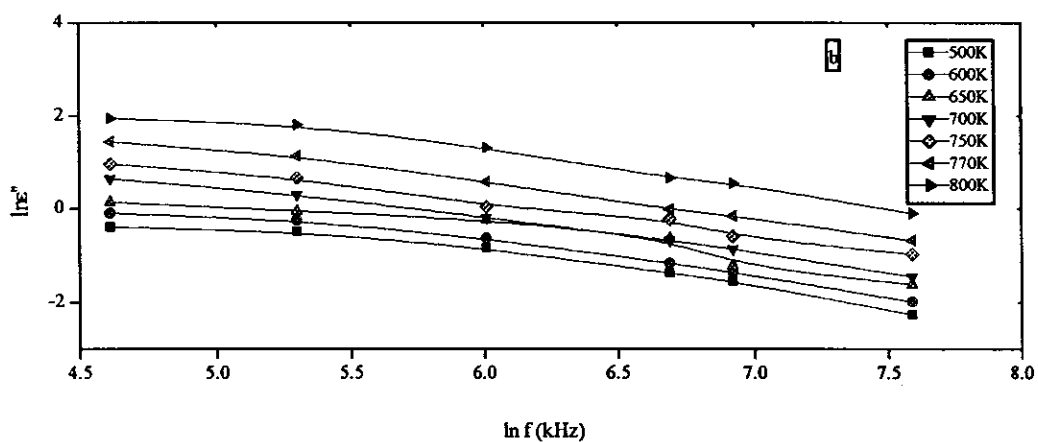
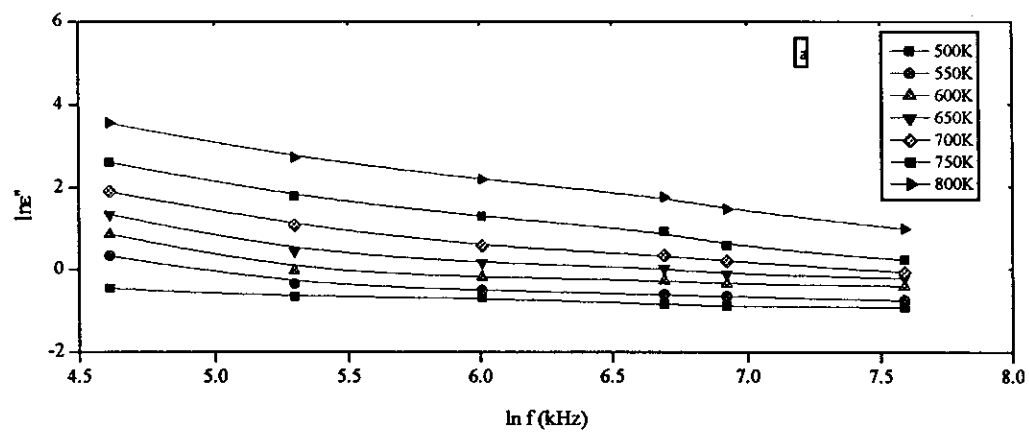


Fig. (3.17: a-c): Frequency Dependence of the Dielectric loss factor ( $\epsilon''$ )

at different fixed temperature for a:(S3), b:(S5) and c:(S6).

Table (3.9): The values of Exponent (m) for the samples  $[0.25(X_2O). 0.53 (SiO_2). 0.08 (Bi_2O_3). 0.14 (B_2O_3)]$ , where X= (Na (S3), Ag (S5) and K (S6)), at different temperature.

Temperature (K)	S3	S5	S6
500	0.161	0.641	0.680
550	0.333	0.680	0.697
600	0.378	0.589	0.831
650	0.412	0.589	0.895
700	0.644	0.660	1.007
750	0.926	0.564	1.057
800	0.849	0.802	1.109

Table (3.10): The obtained values of the liberating Energy ( $W_m$ ) (eV) for different samples and temperature of glass system

Temperature (K)	S3 ( $10^{-20}$ )	S5 ( $10^{-20}$ )	S6 ( $10^{-20}$ )
500	10.2	4.30	4.06
550	9.13	4.87	4.36
600	8.77	6.09	3.98
650	8.72	6.09	4.01
700	6.00	6.28	3.66
750	4.47	7.54	3.73
800	5.20	5.50	4.39

From another point of view, if an alternating electric field is applied for the samples, the dipoles can follow the change of the field direction only if the pairs can reorient quickly enough. Since the

reorientation involves the jumping of charges into the vacancies, they can only follow alternating field of frequency ( $f$ ) less than the jump rate ( $p$ ). For  $f > p$  the pairs do not contribute to the relaxation permittivity. When the frequency  $f$  is nearly equal to the rate  $p$ , there is a phase lag between the applied field and the polarization of the glass, therefore the energy absorbed reaches its optimum value. For all samples the mentioned range of temperature and frequency show dispersion in  $\epsilon''$  which suggests that the ionic relaxation decreases with increasing frequency. The ionic relaxation may depend on the activation energy required for crossing the barriers.

Figure (3-18) shows the temperature dependence of the dielectric loss factor  $\epsilon''$ , at various frequencies for the investigated glass samples. From the figure, it is clear that the values of  $\epsilon''$  increases with increasing temperature except for sample S5, which reveals a slight increase. In addition, the dielectric loss factor  $\epsilon''$  increases when the energy dissipation due to the temperature rises, depending markedly on the type of the participation alkali metal oxide for S3 at low temperature  $\epsilon''$  depend on temperature and independent on frequency, this is completely different with S5, otherwise at high temperature  $\epsilon''$  depends on both temperature and frequency. This trend can resulted from the effect of temperature and frequency together increase the thermal energy to a large rate in which the viscosity begin to decrease. This in terms increases the dipole degrees of freedom and the disturbance occurs in the glass network increasing  $\epsilon''$ .

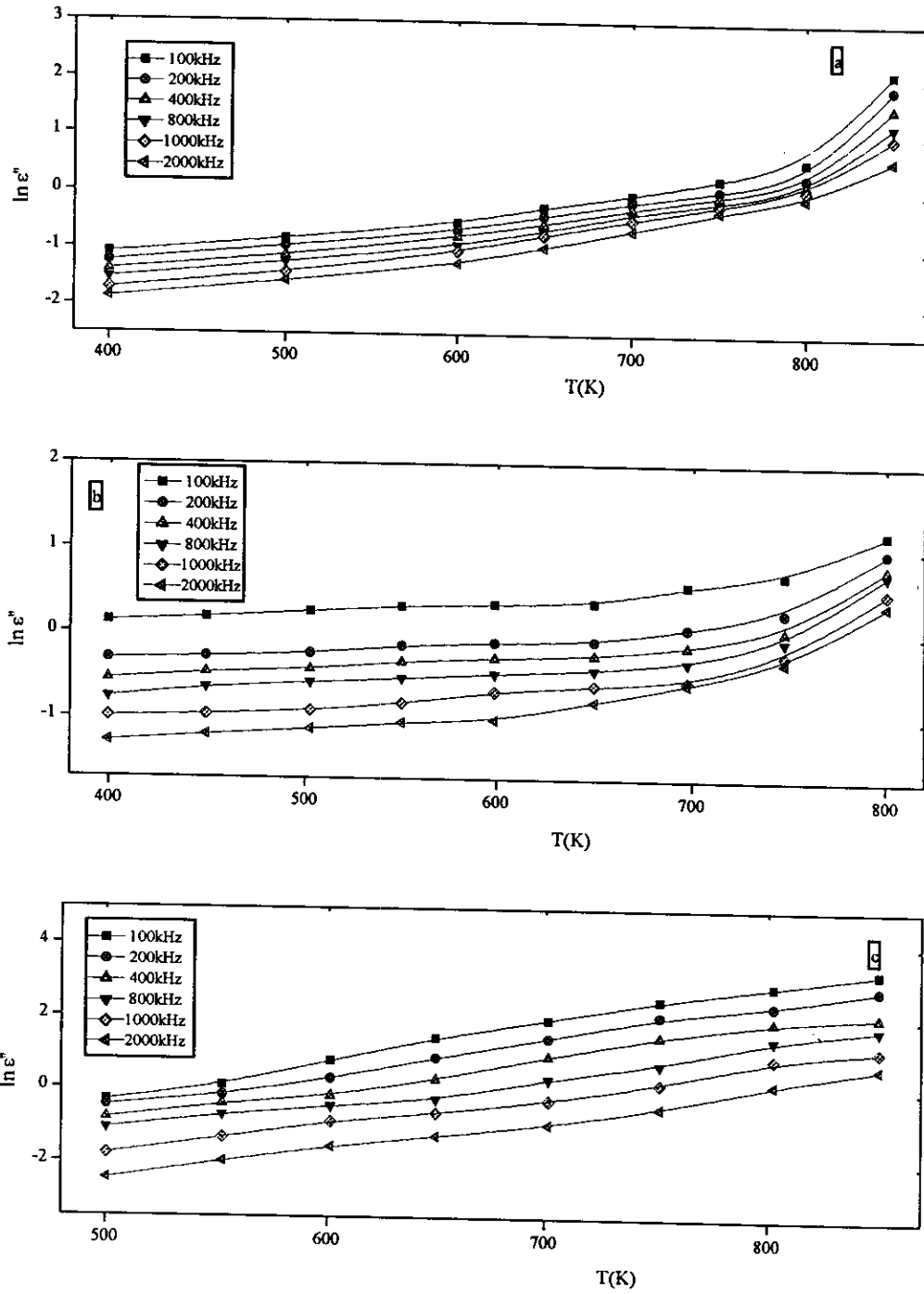


Fig. (3.18): Temperature dependence of the dielectric loss factor ( $\epsilon''$ ) at different frequencies for a:(S3), b:(S5) and c:(S6)).



### 3.3 The Influence of Ion Exchange on I-V Characteristics of Sodium Content in the Silicate Based Glasses

#### 3.3.1 The Effect of Temperature on the I-V Characteristics

The I-V characteristic curves of the glassy samples X (Na<sub>2</sub>O). 0.53 (SiO<sub>2</sub>). 0.08 (Bi<sub>2</sub>O<sub>3</sub>). 0.39-X (B<sub>2</sub>O<sub>3</sub>); X = 0.05(S1), 0.15(S2), 0.25(S3) and 0.35(S4), which treatment by different time of ion exchange (12, 24, 36 and 48h) with silver ion, are studied at different ambient temperatures from 298K up to 393K, the results are shown in Figs. (3.19-22:a-d). The results show that the general behavior for all investigated samples consist of two distinct regions. The off state region (high resistance state at low fields) and the negative differential resistance state (NDR) at high field. The two regions are separated with a turnover point (TOP) which is characterized by differential zero resistance ( $\partial V/\partial I=0$ ). At lower field the conduction current increases with increasing applied voltage obeying ohm's law, after that the current increases exponentially up to the turnover point (TOP) at which the applied voltage drops down to lower value with sharp increase of the current and the differential negative resistance region attains. The voltage and current at (TOP) are known as threshold voltage,  $V_{th}$ , and threshold current,  $I_{th}$ .

The characteristic parameters of switching  $V_{th}$ ,  $I_{th}$ ,  $R_{th} = (V_{th}/I_{th})$ , dissipated threshold power  $P_{th} = (V_{th} \cdot I_{th})$  and  $E_{th} = (V_{th}/d)$  in the conduction path at the turnover point for glass samples under investigation have been calculated and listed in tables (3.11,a-d). The attenuation of the value of the threshold voltage  $V_{th}$  with increasing temperature can be explained based on the electrothermal model <sup>(29)</sup>

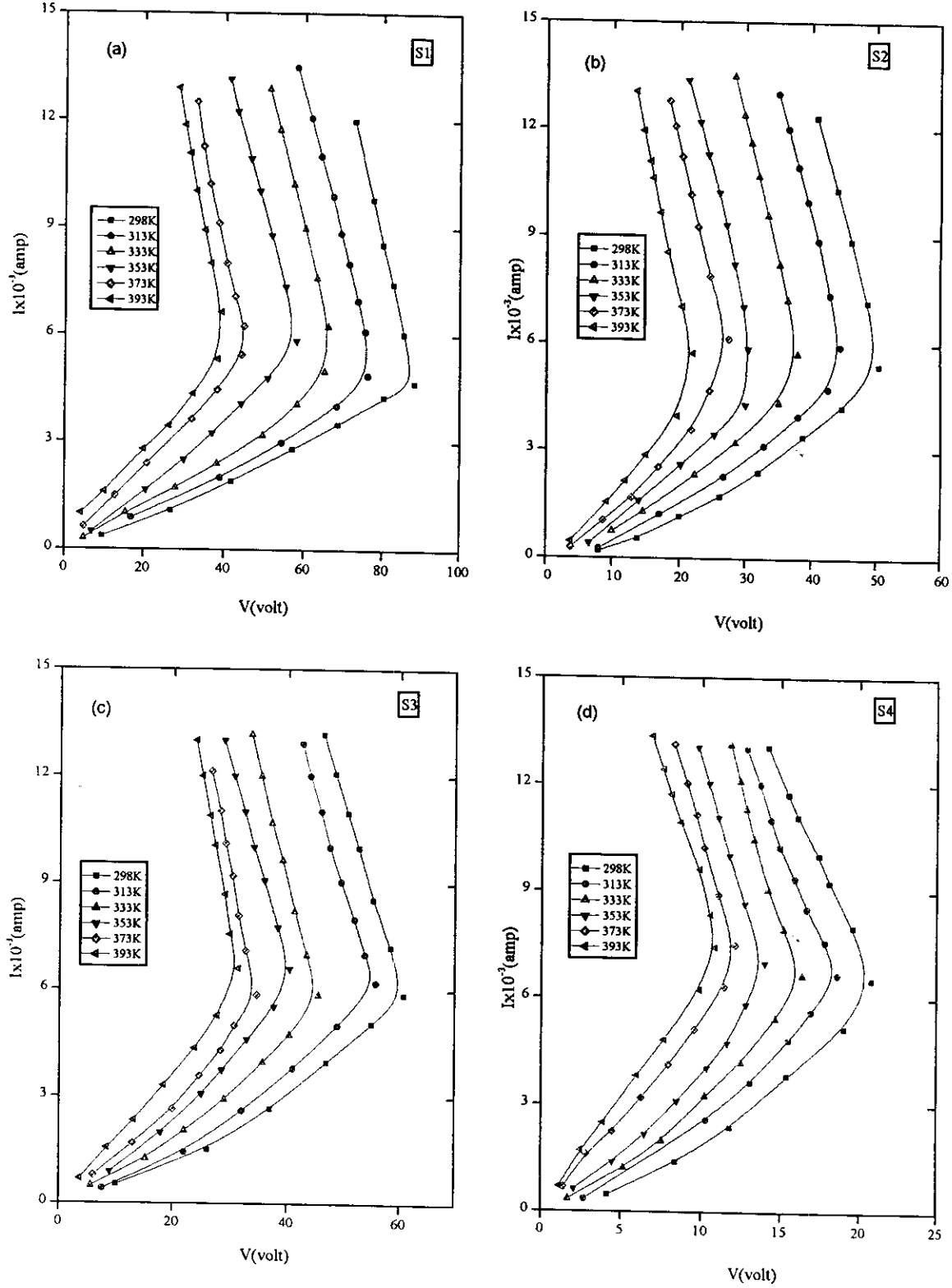


Fig (3.19:a-d): Dependence of the I-V characteristic at different fixed temperatures on the samples  $x(\text{Na}_2\text{O}) \cdot 53(\text{SiO}_2) \cdot 8(\text{Bi}_2\text{O}_3) \cdot 39-x(\text{B}_2\text{O}_3)$ ; [ $x = 5$  (S1), 15 (S2), 25 (S3), 35 (S4)], at time exchange (12)h

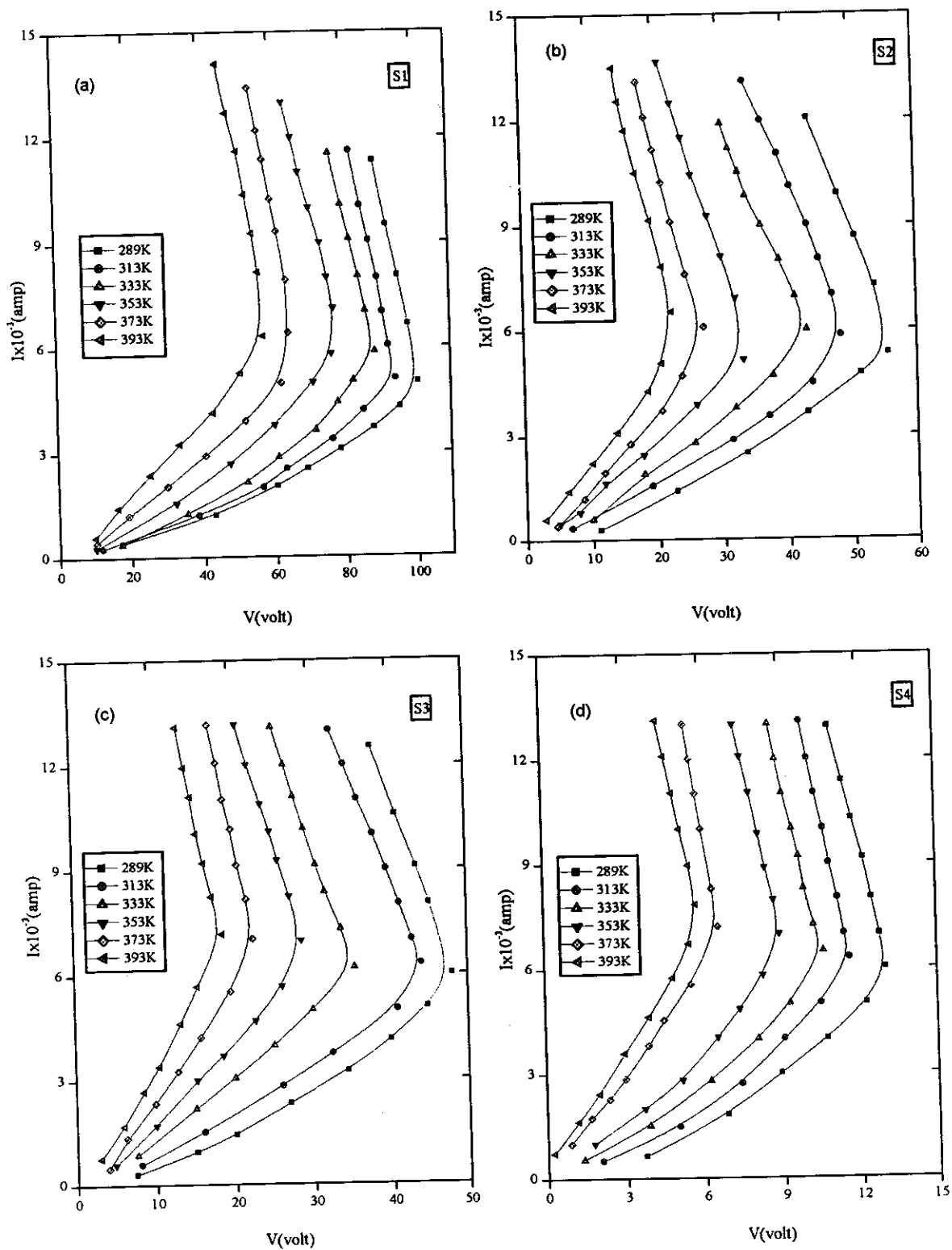


Fig (3.20:a-d): Dependence of the I-V characteristic at different fixed temperatures on the samples  $x(\text{Na}_2\text{O}) \cdot 53(\text{SiO}_2) \cdot 8(\text{Bi}_2\text{O}_3) \cdot 39-x(\text{B}_2\text{O}_3)$ ;  $[x = 5 \text{ (S1)}, 15 \text{ (S2)}, 25 \text{ (S3)}, 35 \text{ (S4)}]$ , at time exchange (24)h

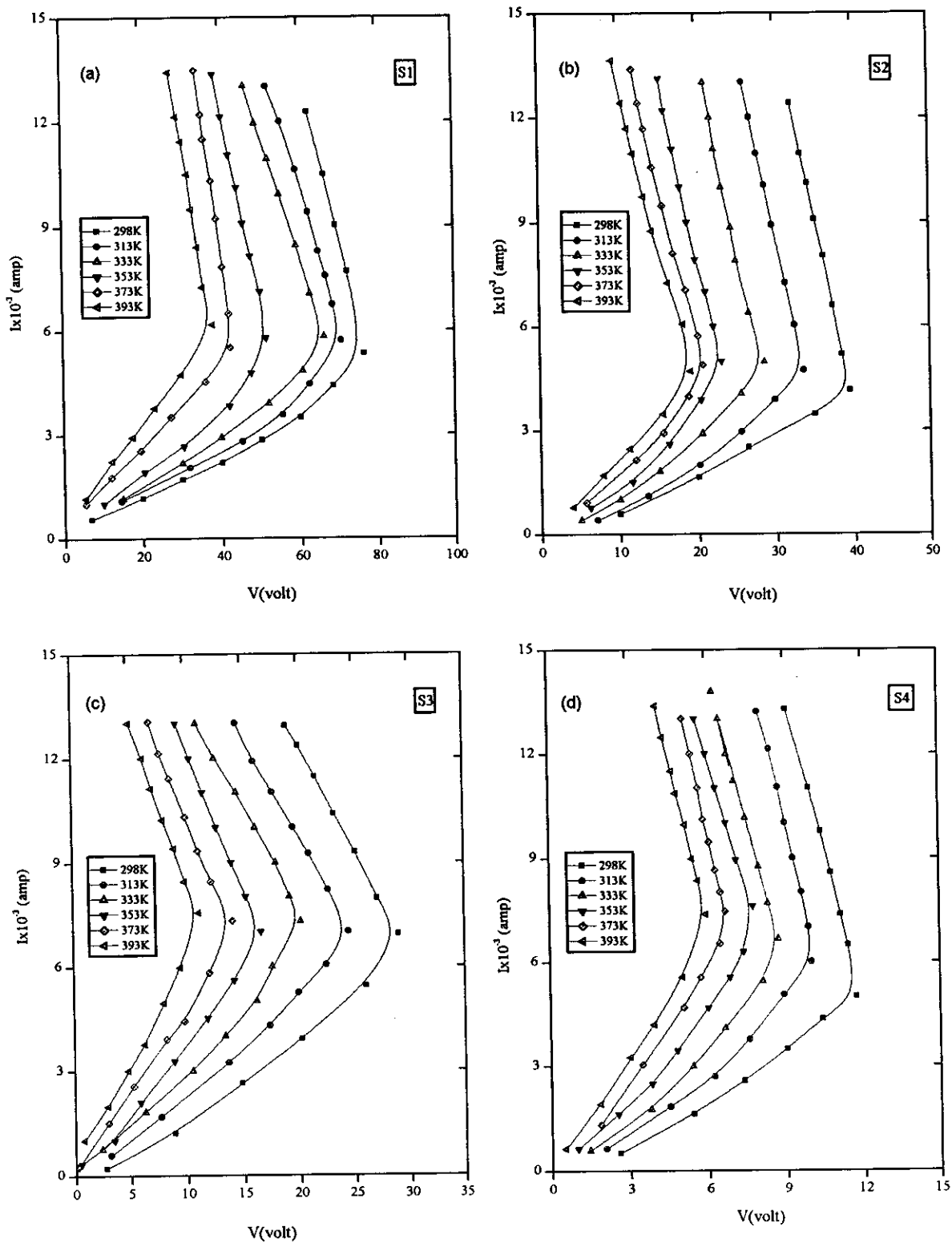


Fig (3.22:a-d): Dependence of the I-V characteristic at different fixed temperatures on the samples  $x(\text{Na}_2\text{O}) \cdot 53(\text{SiO}_2) \cdot 8(\text{Bi}_2\text{O}_3) \cdot 39-x(\text{B}_2\text{O}_3)$ ; [ $x = 5$  (S1), 15 (S2), 25 (S3), 35 (S4)], at time exchange (48)h

Table (3.11a): The switching parameters  $V_{th}$ ,  $I_{th}$ ,  $R_{th}$ ,  $P_{th}$  and  $E_{th}$  at different ambient temperatures for the glassy system S1 [0.05(Na<sub>2</sub>O). 0.53(SiO<sub>2</sub>). 0.08(Bi<sub>2</sub>O<sub>3</sub>). 0.34(B<sub>2</sub>O<sub>3</sub>)]

Time of exchange	Temp. (K)	$V_{th}$ (volt)	$I_{th}$ (mA)	$R_{th}$ (k $\Omega$ )	$P_{th}$ (mw)	$E_{th} \times 10^{-3}$ (V/m)
12(h)	298	88	4.8	18.3	422	55
	313	78	5	15.6	390	48.8
	333	64	5.7	11.2	365	40
	353	54	6	9	324	33.75
	373	43.5	6.5	6.7	283	27.2
	393	37	7	5.3	259	23.1
24(h)	298	100	5	20	500	76.9
	313	94	5.5	17	517	72.3
	333	85.5	6	14.3	513	65.8
	353	78.5	6.2	12.6	487	60.4
	373	59	7.5	7.9	443	45.4
	393	51	8	6.4	408	39.2
36(h)	298	94.5	5.5	17.2	520	59.1
	313	86	5.7	15.0	490	53.8
	333	80	6	13.3	480	50
	353	70.8	6.2	11.4	439	44.3
	373	49.5	6.5	7.6	322	30.9
	393	35.5	6.8	5.2	241	22.2
48(h)	298	76	5.3	14.3	403	54.3
	313	69	5.7	12.1	393	49.3
	333	65	6	10.8	390	46.4
	353	48	6.3	7.6	302	34.3
	373	38	6.5	5.9	247	27.1
	393	32.6	6.6	4.9	215	23.9

Table (3.11b): The switching parameters  $V_{th}$ ,  $I_{th}$ ,  $R_{th}$ ,  $P_{th}$  and  $E_{th}$  at different ambient temperatures for the glassy system S2 [0.15(Na<sub>2</sub>O). 0.53(SiO<sub>2</sub>). 0.08(Bi<sub>2</sub>O<sub>3</sub>). 0.24(B<sub>2</sub>O<sub>3</sub>)]

Time of Exchange	Temp. (k)	$V_{th}$ (volt)	$I_{th}$ (mA)	$R_{th}$ (k $\Omega$ )	$P_{th}$ (mw)	$E_{th} \times 10^{-3}$ (V/m)
12(h)	298	50.5	5.4	9.4	273	36.1
	313	44	5.5	8.0	242	31.4
	333	38	5.7	6.6	217	27.1
	353	30	5.8	5.2	174	21.4
	373	21.7	6.8	3.2	148	15.5
	393	16	6.9	2.3	110	11.4
24(h)	298	56	5.4	10.4	302	50.9
	313	48	5.8	8.3	278	43.6
	333	43	6	7.1	258	39.1
	353	27.6	6.2	4.5	171	25.1
	373	21	6.5	3.2	136	19.1
	393	18	6.7	2.7	121	16.4
36(h)	298	46	5	9.2	230	30.7
	313	42	5.5	7.6	231	28
	333	36	6	6	216	24
	353	25	6.2	4.0	155	16.7
	373	21	6.5	3.2	136	14
	393	16.6	6.6	2.5	110	11.1
48(h)	298	39.5	4	9.9	158	39.5
	313	33.6	4.7	7.2	158	33.6
	333	28.6	5	5.7	143	28.6
	353	23	5.2	4.4	120	23
	373	17	5.5	3.1	94	17
	393	12	5.7	2.1	68	12